The atypical transport system

Natural gas pipeline system

Yang, Zhaoming; Xiang, Qi; He, Qian; Faber, Michael H.; Zio, Enrico; Su, Huai; Zhang, Jinjun

Published in:
Energy Reports

DOI (link to publication from Publisher):
10.1016/j.egyr.2023.12.047

Publication date:
2024

Document Version
Publisher's PDF, also known as Version of record

Energy Reports 11 (2024) 791–816

Contents lists available at ScienceDirect

Energy Reports

journal homepage: www.elsevier.com/locate/egyr

Research paper

The atypical transport system: Natural gas pipeline system

Zhaoming Yang [a], Qi Xiang [a], Qian He [a], Michael H. Faber [d], Enrico Zio [b,c], Huai Su [a,*], Jinjun Zhang [a,*]

[a] National Engineering Laboratory for Pipeline Safety/MOE Key Laboratory of Petroleum Engineering/Beijing Key Laboratory of Urban Oil and Gas Distribution Technology, China University of Petroleum-Beijing, 102249 Beijing, China
[b] MINES ParisTech, PSL Research University, CRC, Sophia Antipolis, France
[c] Dipartimento di Energia, Politecnico di Milano, Via La Masa 34, 20156 Milano, Italy
[d] Department of the Built Environment, Aalborg University, Aalborg, Denmark

ARTICLE INFO

Keywords:
Natural gas pipeline system
Self-organized criticality
Power law
R/S analysis
Small world network

ABSTRACT

The natural gas pipeline system (NGPS) is complex with a diverse network topology. This study elucidates the network characteristics of the NGPS, revealing that it shares commonalities with small-world networks, but with differences caused by its structural and operational characteristics. The combination of the low aggregation effect caused by branching structure and the offsetting effect caused by economic and geographical constraints results in a network with small world characteristics. NGPS has longer mean path than common small world network, but the aggregation factor is close to that of a standard small world network. With respect to its small-world characteristics and correlation with self-organized criticality (SOC), an in-depth study of the SOC characteristics of the NGPS was conducted utilizing a combination of traditional logarithm analysis and R/S analysis. The findings establish that there are atypical SOC characteristics, characterized by a weakened power law within a specific functional range, thereby encouraging the advancement of SCADA and other safety technologies. Because of the line-pack, which induces time lags in the NGPS, NGPS can prevent the cascade failures. The reasons for the periodicity and centrality of NGPS data are analyzed by the affecting components, with the R/S analysis verifying a weak positive correlation of the function data across different time series. The interlinking of the SOC and R/S analysis illustrates the connection between critical status, accident type, and operation index. The results prove the reasonability and importance of insurance measures, such as regular internal detection, higher grade steel pipes change and staff training et al., in a novel view of SOC. The future works in building accidents database and human factors study are proposed.

1. Introduction

The complexities of NGPS are reflected in network topology and system dynamics. As an energy transportation system, the topology and state of system are important to NGPS safety, operation and maintenance. Similar with power grid and traffic roads system, the topology of NGPS is complex network, and analyzing topology with complex network theory and graph theory are basics of NGPS research. In addition, criticality state is the hotspot in system science and complexity science, which is necessary and important for complex industrial system operation and prewarning. (Dorogovtsev et al., 2007; Jun et al., 2023; Chenhui et al., 2021).

1.1. Self-organized criticality

It should be clarified that the Self-organized Criticality (SOC) still has disputes and there has not been a universally acceptable definition (Bak et al., 1987; Shi and Liu, 2009). Researchers have tried to derive the strict mathematical expression, but failed. The SOC theory is aimed to show the relationship between the scales of disasters or disruption events and the corresponding frequency. Brookhaven national laboratory, which is the presenter of SOC theory (American et al., 1991; Bak, 1990; Bak et al., 1988; Mauro et al., 2018; Najafi and Tizdast, 1999; Sethna, 2022), used sandpile model to the process of to-criticality and criticality (Bak et al., 1987).

The SOC system generally fits a power-law distribution, which is to describe the trends of emergencies and fluencies. The function can be

* Corresponding authors.
E-mail addresses: suhuai@cup.edu.cn (H. Su), zhangjj@cup.edu.cn (J. Zhang).

https://doi.org/10.1016/j.egyr.2023.12.047
Received 4 July 2023; Received in revised form 12 December 2023; Accepted 20 December 2023
Available online 26 December 2023

Table 1
The researches of System and SOC.

Researcher	Year	System type	Measuring index	Reference
Yousef Heider	2022	Fracture modeling	Fracture width	(Heider et al., 2022)
John C. Mauro	2018	Safety system	Workplace accident frequency	(Mauro et al., 2018)
B. Dupoyet	2011	Financial markets	Statistical properties	(Dupoyet et al., 2011)
Jun-fang Li	2012	Optimization algorithms	Spatial evolution character	(Li et al., 2012)
Hong-Li Zeng	2020	Neural networks system	The power spectrum of return time	(Zeng et al., 2020)
Alexander V. Milovanov	2021	Extreme events	Prediction degree	(Milovanov et al., 2021)
Kai Shi	2009	Air pollution	Air pollution indexes	(Shi and Liu, 2009)
Akira Kato	2020	Forest system	Fire size	(Kato et al., 2020)
M. Paczuski	2004	Solar system	Magnetic field energy	(Paczuski and Hughes, 2004)
Gui-Qing Zhang	2009	Earthquake system	The real seismic data	(Zhang et al., 2009)
J.C. Phillips	2012	Mutated protein	Transportational survival rates	(Phillips, 2012)
Donald L. Turcotte	2004	Natural hazard	Landslide probability	(Turcotte and Malamud, 2004)
Roberto N. Onody	2003	Optimization algorithm	Dynamics performance	(Onody and De Castro, 2003)
Di Lu	2007	Economic system	M traits	(Lu and Du, 2007)
João P. da Cruz	2012	Network of economic agents	Return of macroscopic quantities	(Da Cruz and Lind, 2012)
J.C. Sprott	2002	Forest system	Forest-landscape evolution	(Clar et al., 1999)
Ferenc Pázmándi	2000	Random ferromagnets	Hysteretic phenomena	(Pázmándi et al., 2000)
Weiguo Song	2001	Forest system	Fire frequency	(Song et al., 2001)
M.A. Moret	2011	Protein system	Protein folding	(Moret, 2011)
K. Bhattacharya, S.S. Manna	2007	Earthquake	Magnitudes of earthquakes	(Bhattacharya and Manna, 2007)
H. Saba	2014	Epidemic system	The number of dengue cases	(Saba et al., 2014)
Xingyong Zhao	2009	Power system	Blackout size	(Zhao et al., 2009)
Heiko Hoffmann	2014	Model of non-contiguous cascading failures	Event sizes	(Hoffmann and Payton, 2014)

described as

$$N(x) = ax^{-k} \tag{1}$$

where N is the number of occurrences or frequency of an event in scale x, a is a proportionality factor, and k is a scaling exponent. The power-law distribution fits a characteristic straight line when plotted in log–log axes, i.e., when plotting the logarithm of the number of occurrences and the logarithm of the avalanche size, shown as

$$\log N = \log a - k \log x \tag{2}$$

In a log–log plot, the slope of the line reveals the value of the scaling exponent k. The Eq. (2) can quantitively show that the accidents with larger effects are in low possibility. The first key point of SOC is balance. The SOC system operates in balance, due to the sizes and types of different systems, the balances and their degree of closeness to criticality are different. If the present balance is disrupted, the system can change into a new balance or try to keep the original state, and this process can finish by the system. The second key point is disturbance. It is a related concept to the resilience of the system. There is no system which is indestructible, and the disturbance which can bring the system into criticality or even collapse depends on the level of that and the over-measure of the system. The third key point is criticality. For a SOC system, the criticalities differ from different levels of damages. The game between criticality and disturbance affects the balance of system. For engineering area, the importance of SOC is to build a bridge between disturbance events and the possibility of happening, so as to provide constructive advice on the pre-warning and resilience improvement.

1.2. Systems and SOC

Many systems have the characteristics of SOC, with the scales of systems changing from nanometers such as kinds of materials crack (Heider et al., 2022; Jensen and Magnasco, 1999), to the whole ecosystem(Da Cruz and Lind, 2012; Dupoyet et al., 2011) or solar system (Paczuski and Hughes, 2004). Table 1 has summarized the SOC research based on different systems. The application areas of SOC have been physics, biology, geosciences, economics, and the social sciences. For forest system, SOC theory can quantify the fire size and frequency, in order to predict the trend of fire activity(Clar et al., 1999; Kato et al., 2020; Song et al., 2001). In addition, some natural disasters (Turcotte and Malamud, 2004) such as landslides and earthquakes (Bhattacharya and Manna, 2007), including earthquake magnitudes distribution, have their own possibility and size models, which fit the SOC characteristics. The SOC theory is also applied in the material crack modelling (Bernardes and Moreira, 1995; Ebrahem et al., 2020; Heider et al., 2022; Huang et al., 2013), and prove the presence in both macroscopic and microscopic. For the social science research, the workplace accidents (Mauro et al., 2018; Nielsen, 2014; Shannon et al., 1997; Turcotte and Rundle, 2002) fit a power law with their severity as measured by the number of days from lost work. The financial market also has the characteristics of SOC (Dupoyet et al., 2011, 2010; Feigenbaum, 2003; Poon and Granger, 2003), which is seen as the internal driving mechanism and applied for the market modelling. The operation of a firm is studied and the characteristics are also described as SOC. For the biology research, the brains of human beings are supposed to be a SOC system, and the theory can simulate the threshold firing and refractory periods as the key features of neurons. The process of protein folding is also seen as the SOC process (Moret, 2011; Phillips, 2012). The air pollution is also thought as a SOC system, which shows the minor air pollution sources can trigger the occurrence of large pollutant events by SOC behavior (Adamic and Huberman, 2000; Barabási and Albert, 1999; Chessa et al., 1998; Shi and Liu, 2009). Similarly, the evolution of disease, such as dengue disease in cities, is studied by following the SOC theory (Saba et al., 2014). The magnetic field network in the corona and its burst have the characteristics of SOC in the size and frequency (Onody and De Castro, 2003). In the view of energy system, the power grids are equipped with the SOC characteristics, with the long-time dependencies. The research of power grids from many countries can guide the prediction in large blackouts or better control of power grids (Milovanov et al., 2021; Onody and De Castro, 2003; Zhao et al., 2009).

In addition, SOC theory has also been applied in algorithms optimization, such as Genetic Algorithm, Differential Evolution and the Artificial Immune System algorithm. For the SOC itself modification, a weighted Olami, Feder, and Christensen (OFC) model is applied to improve the redistribution rule of original SOC model (Marković and Gros, 2014). Some researchers think that SOC theory can not fully explain the characteristics of systems, so the scaling function, the distribution of energy fluctuations, the distribution of inter-event waiting times, and other higher order spatial and temporal correlations are proposed to characterize the systems.

However, the researches show that SOC theory has contributed much to the safety of energy systems, especially to the power grids. NGPS plays a key role in energy system, but few research prove that NGPS has the

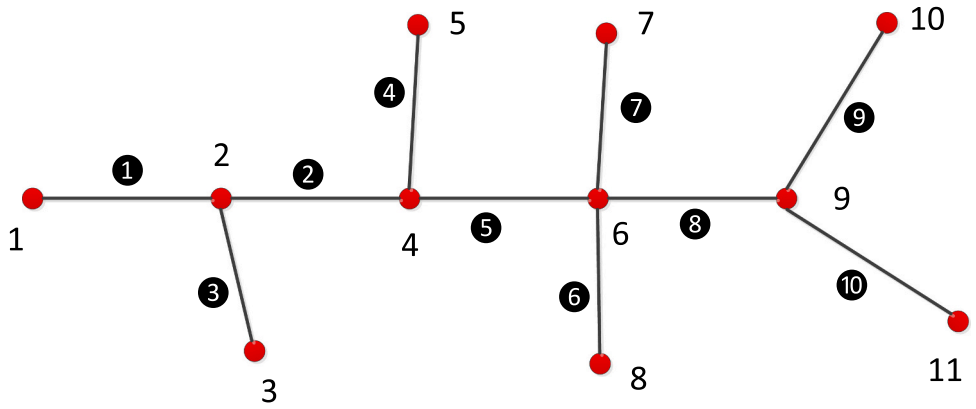

Fig. 1. A case of pipeline network.

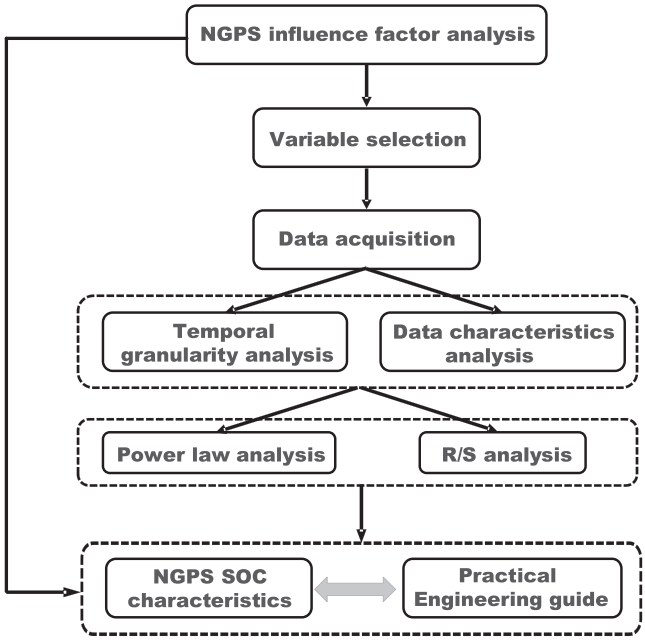

Fig. 2. Methodology and logical order.

characteristics of SOC. This paper explores the relationship between NGPS and SOC, also discusses the contribution of SOC to the NGPS engineering operation.

1.3. Network theory and small world networks

The networks can be classified by three types of criteria, the first of which is the classification of complex networks into homogenous networks, whose degrees are approximately the same, and heterogeneous networks, whose degrees obey a certain distribution. Secondly, it can also be divided into undirected and directed networks based on the directionality of the edges in the network (Boccaletti et al., 2006). Typical undirected networks that have been studied include the Internet (Caldarelli et al., 2000; Pastor-Satorras et al., 2001), collaborative networks of scientists (Barabā et al., 2002; Newman, 2001), and collaborative networks of film actors (Albert and Barabási, 2000). Typical directed networks include: intracellular chemical reaction networks (Fell and Wagner, 2011; Jeong et al., 2000), food chain networks (Camacho et al., 2002b, 2002a; Dunne et al., 2002; Williams et al., 2002), citation networks (Redner, 1998), and power networks (Albert et al., 2004; Carreras et al., 2002). When we ignore the directionality of the interrelationships between nodes, the directed network becomes an undirected network. Another classification method is to classify complex networks into weighting networks and unweighted networks based on whether the weights of the edges are considered, usually using the length of the edges between the nodes as the weights.

In 1998, Watts and Strogatz proposed the small world network model (WS model), which introduced randomness into regular networks and provided a new way to describe network systems (Strogatz, 2001). Based on that, navigation networks, airline networks, and urban roads have shown the similar network characteristics, for example, the rail networks in Boston and India have shown small world network characteristics (Albert et al., 2004; Carreras et al., 2002). With the further development of small world network research, its evolutionary mechanism (Amaral et al., 2000), discriminant criterion (Barrat and Weigt, 2011), scope and form of existence (Telesford et al., 2011) have been further clarified. Based on these findings, the relationship between small world networks and SOC properties has also been further investigated. It has been shown that the artificial small world networks have SOC characteristics by simulation. (De Arcangelis and Herrmann, 2002). On the basis of this research, network models such as social balance dynamics have also been shown to have SOC properties, so the relation between SOC and small world has also started to be revealed.

In summary, based on the relationship between small world networks and SOC, this paper studies the small world properties of NGPS at first, and the results of that supply the idea to further explore the SOC characteristics. Both of them prove the atypical properties of NGPS. The main contributions of this article are analyzing the complexity of NGPS in view of networks topology and system dynamics. Based on the NGPS topology, it is proposed that NGPS has small world characteristics which are different from original theory. Based on system dynamics, the special SOC characteristics are studied. It has been proved that NGPS is a complex and atypical industrial system. The results explain reasons for the particularity, which is helpful to the further understanding of NGPS construction and safety.

2. Methodology

2.1. Network description

Branches are generally considered to be the simplest structural unit of NGPS. However, this study explores the division of the minimum structural unit of a pipeline network, by using the degree of connected nodes as a criterion to classify the structure. By counting the subdivided structures, whether the NGPS has specific structural characteristics is studied.

As shown in Fig. 1, the network has a total of 11 nodes and 10 edges. Looking at the structure, it can be seen that the nodes at the end of edge 1 are node 1 and node 2, with node 1 having a node degree of 1 and node 2 having a node degree of 3. In this paper, such a structure is defined as

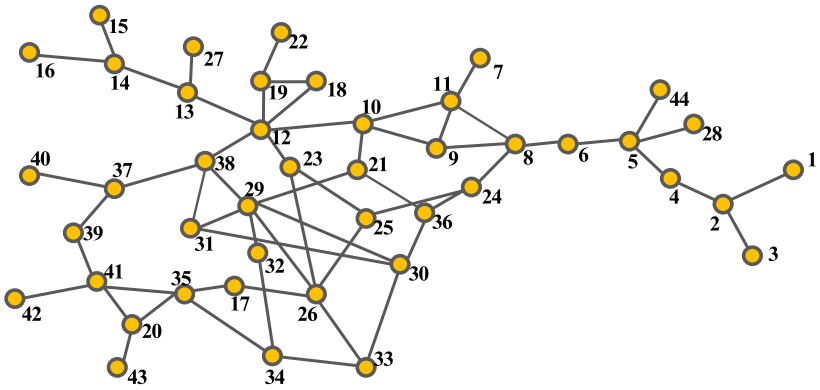

(a) NGPS topology of case A

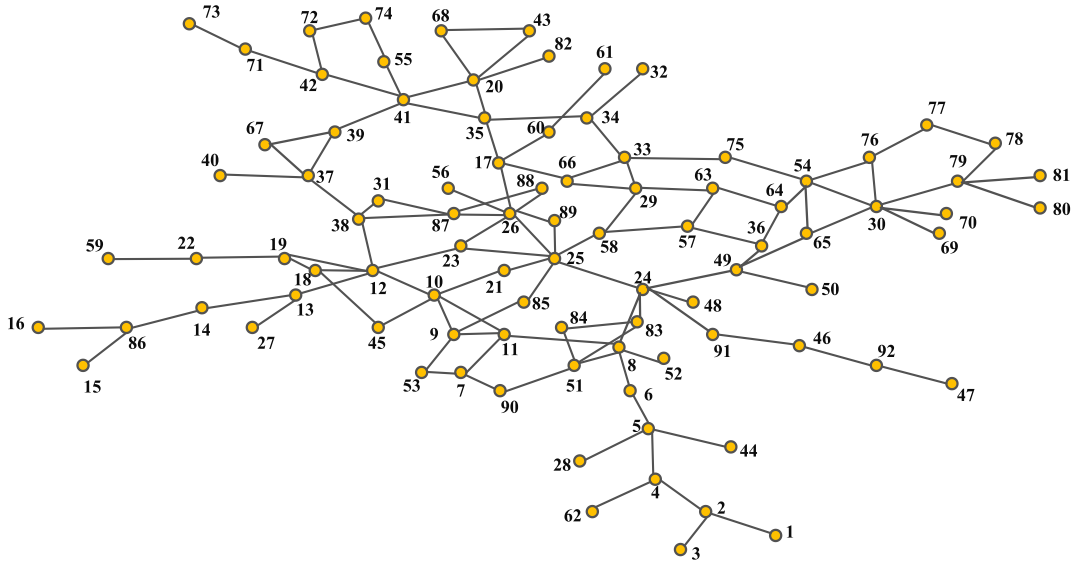

(b) NGPS topology of case B

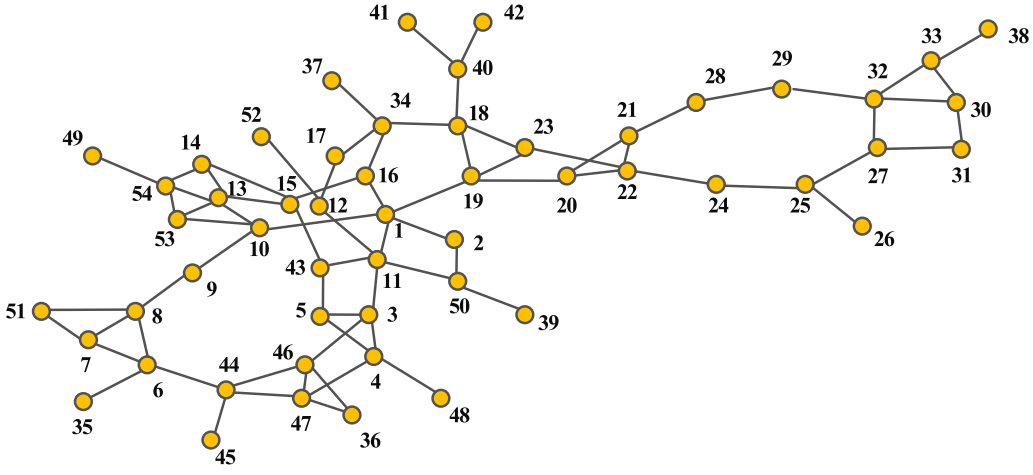

(b) NGPS topology of case C

Fig. 3. The network model diagram of natural gas pipeline network.

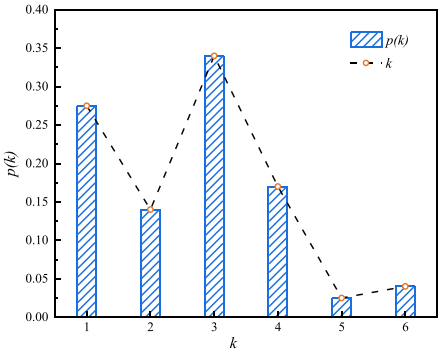

(a) Degree distribution of case A

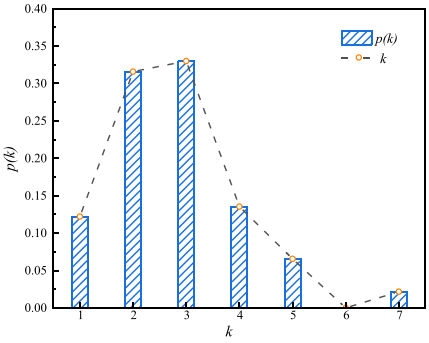

(b) Degree distribution of standard small world network

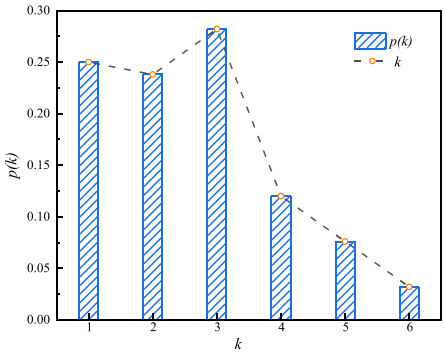

(c) Degree distribution of case B

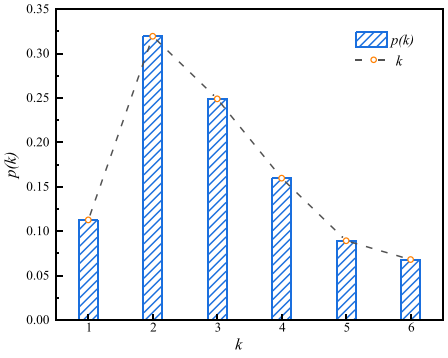

(d) Degree distribution of standard small world network

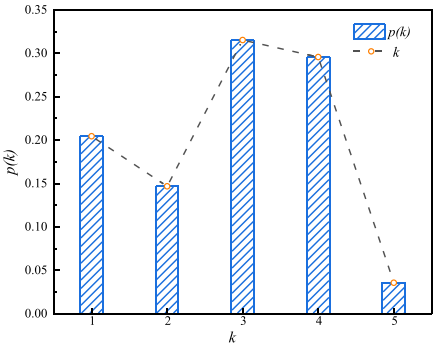

(e) Degree distribution of case B

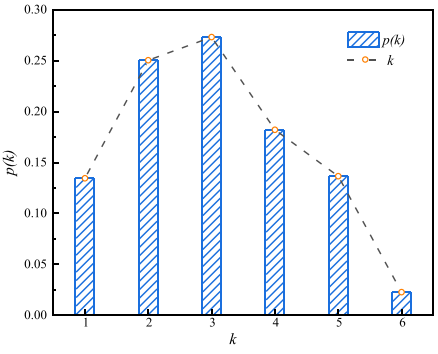

(f) Degree distribution of standard small world network

Fig. 4. Comparison of degree distribution between NGPS and small world network.

1–3, where 1–3 and 3–1 are equivalent. Similarly, the two end nodes of edge 8 are node 6 and node 9. node 6 has degree of 4, while node 9 has degree of 3. Such a structure is 3–4. The structural characteristics in the case can be known by analyzing the proportion of each structure.

2.2. Network analysis

Realistic networks are both deterministic and probabilistic, usually with high aggregation coefficients and small mean path lengths, which are not well described by either regular or random networks. The small world network model introduces randomness into a regular network, and uses the regular network as a basis for generating new connected edges with probability P after removing edges from the network. The WS model is a typical small world network model that evolves as follows:

(1) Constructing a rule graph. A network containing N nodes is constructed, with N nodes enclosed in a loop, and any node on the

Table 2
The statistical description value information table of different network.

Network	Natural gas pipeline network (A)	Random network	Regular network	No scale network	Small world network A	Small world network B
Average degree	2.58	2.54	4	2.15	4	4
Degree distribution pattern	Bell-shaped distribution	Poisson distribution	Single point	Power law distribution	Bell-shaped distribution	Bell-shaped distribution
Aggregation factor	0.10	0.03	0.75	0.02	0.07–0.16	0.37–0.45
Average path length	5.82	4.77	11.5	4.62	3.47–3.61	4.89–6.08

Table 3
The structure information table of the small world network A.

Structure	Percentage (%)	Structure	Percentage (%)
2-3	0.01	2-4	0.01
2-5	0.01	3-3	0.01
3-4	0.13	3-5	0.02
4-4	0.53	4-5	0.23
4-6	0.03	5-5	0.02

Table 4
The clustering coefficient information table of the small world network A.

Node aggregation coefficient values	Percentage of total nodes (%)
0	2
0.17	8
0.5	49

Table 5
The structure information table of the small world network B.

Structure	Percentage (%)	Structure	Percentage (%)
2-3	0.01	2-4	0.02
2-5	0.03	2-6	0.01
2-7	0.01	3-3	0.08
3-4	0.14	3-5	0.05
3-6	0.08	3-7	0.03
4-4	0.18	4-5	0.08
4-6	0.16	5-5	0.02
5-6	0.07	5-7	0.02
6-6	0.03	6-7	0.02

Table 6
The clustering coefficient information table of the small world network B.

Node aggregation coefficient values	Percentage of total nodes (%)
0	59
0.17	13
0.5	0

Table 7
The structure information table of natural gas pipeline network.

Structure	Percentage (%)	Structure	Percentage (%)
1-3	0.07	1-4	0.05
2-3	0.08	2-4	0.06
2-5	0.05	2-6	0.02
3-3	0.08	3-4	0.22
3-5	0.03	3-6	0.03
4-4	0.03	4-6	0.03
5-6	0.02	1-5	0.03
1-2	0.03	2-2	0.06
1-6	0.03	2-6	0.02
2-5	0.05	4-5	0.04

Table 8
The clustering coefficient information table of natural gas pipeline network.

Node aggregation coefficient values	Percentage of total nodes (%)
0	74
0.17	5
0.5	0

ring is edged with each of its nearest $K/2$ nodes, where K is an even number.

(2) Random reconnection. An edge in the regular graph is selected randomly to unlink two nodes, one of which is selected and the other is chosen from N-K-1 nodes. Whether two nodes can be connected to an edge is related to the probability P.

When $P = 0$, the original network does not change and remains a regular network; when $P = 1$, every edge in the original network will go through the process of deletion and reconstruction, changing into a random network. The evolutionary mechanism of small world networks is the introducing of randomness into regular networks, giving them a high aggregation factor and a small average path length.

The structural characteristics of complex networks can be shown in the corresponding statistical indexes, and the statistical indexes used in this paper are shown as:

①Node degree.

Node degree is a statistical descriptive value that measures the importance of a node at the topological connectivity level. In an undirected graph, the number of nodes directly connected to node v_i is defined as its node degree k_i, and the average degree of all nodes in the network reflects the complexity of the network structure, denoted as $\langle k \rangle$, as shown in Eq. (3):

$$\langle k \rangle = \frac{1}{N} \sum_{i=1}^{N} k_i \tag{3}$$

where N is the number of nodes in the network.

The distribution function $p(k)$ of node degrees in a network represents the number of nodes with degree k as a proportion of all nodes in the network, which is a macroscopic statistical description of the network. Different networks correspond to different degree distributions, for example, the degree distribution of a random network satisfies a Poisson distribution, the degree distribution of a scale-free network satisfies a power-law distribution, and the degree distribution of a small world network has a bell-shaped distribution.

②Aggregation factor.

The aggregation factor is a statistical descriptor of the closeness and efficiency of a network. The aggregation factor c_i for node v_i is defined as the ratio of the actual number of edges k_i connecting directly to the theoretical number of edges e_i, as shown in Eq. (4):

$$c_i = \frac{1}{N} \sum_{i \in N} \frac{2e_i}{k_i(k_i - 1)} \tag{4}$$

where N is the number of nodes in the network.

And the global aggregation coefficient C of the network is defined as the average of the aggregation coefficients, as shown in Eq. (5):

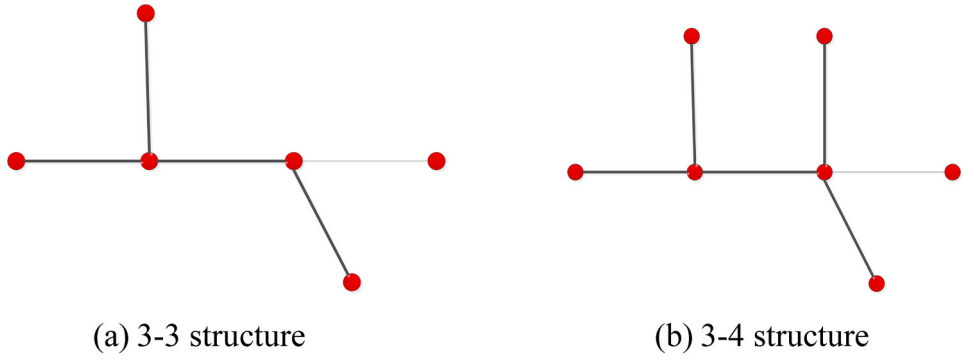

Fig. 5. 3–3 structure and 3–4 structure diagram.

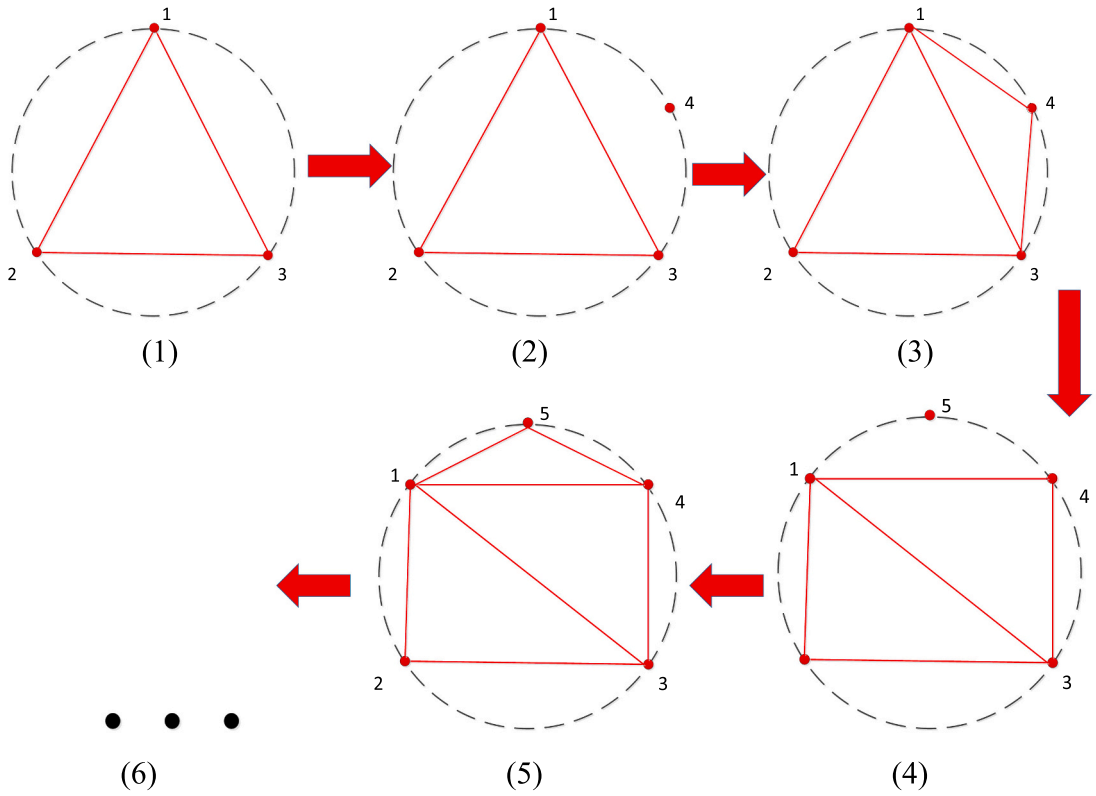

Fig. 6. The schematic diagram of dynamic network model.

$$C = \frac{1}{N}\sum_{i=1}^{N} c_i \tag{5}$$

③Average path length:

The average path length is a statistically descriptive value that measures how close the nodes are to each other. The distance between any pair of nodes in a complex network is defined as the shortest path between pairs of nodes, and the average path length of a network is defined as shown in Eq. (6):

$$L = \sum_{i,j\in V} \frac{l_{ij}}{N(N-1)} \tag{6}$$

where N is the order of the network, l_{ij} is the distance between nodes i and j, and V is the set of nodes of the network.

It should be explained that Eq. (3) defines the node degree k. In practical engineering, the nodes can be stations or pipe connections, such as a distribution station or a user NGPS. The degree represents the total number of pipelines connected to the corresponding node in the network. For Eq. (4), e_i denotes the number of pipes between the neighbor nodes of i. In reality, c_i is aimed to measure the relation between corresponding stations and other stations, which are connected by pipes. For Eq. (5), C is used to measure the overall relations between the kinds of stations in a NGPS. Regarding Eq. (6), this equation serves as a measure of the distance between nodes within NGPS. However, the distance is not the practical length between stations, but the number of pipelines.

2.3. logarithmic analysis

As the components of natural gas are complex and different, due to the different gas sources, the calorific values are different, even in the same volume flow. So the data applied the calorific value measurement method and the units are unified by kWh. Since the fractal theory is a common form of expression, the definition of fractal theory is applied in NGPS SOC analysis. According to the fractal theory, the Eq. (1) is

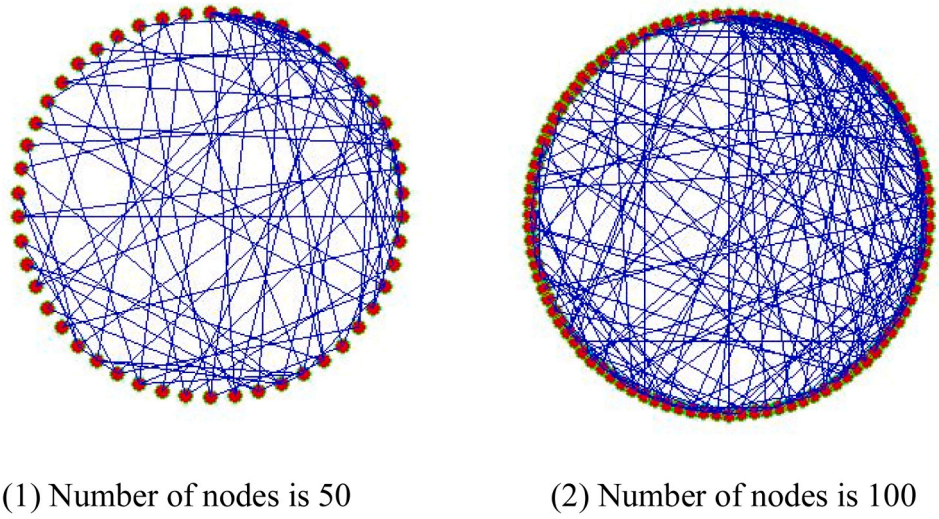

Fig. 7. Model simulation network diagram.

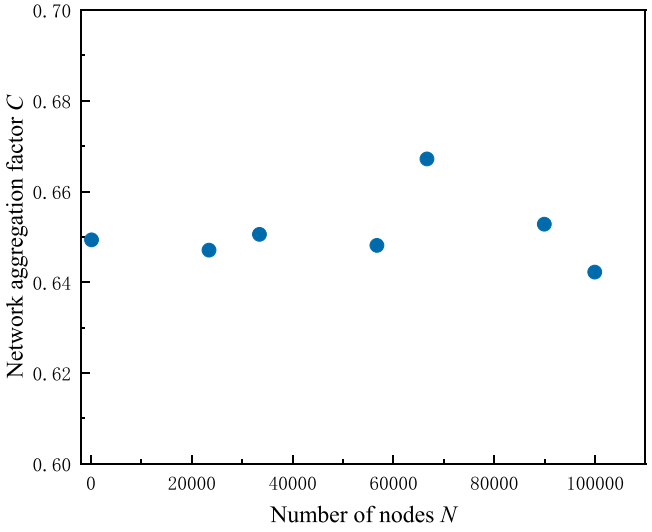

Fig. 8. Clustering coefficient distribution diagram.

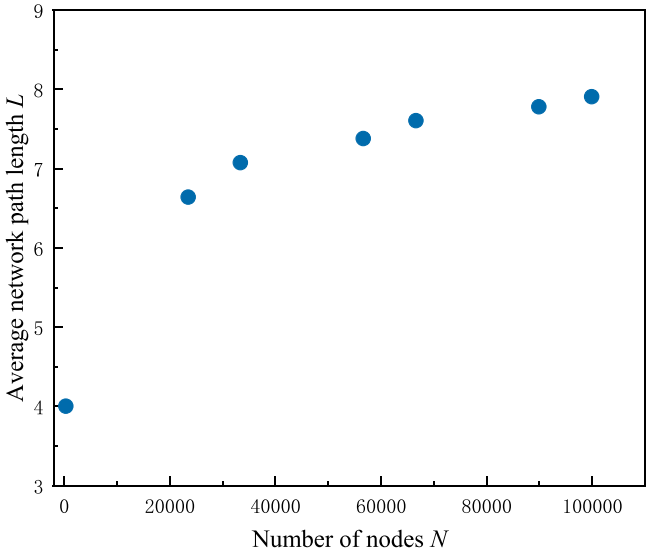

Fig. 9. The average path length distribution diagram.

modified and the object scale r is changed into gas flow which shows the operation condition of NGPS, and the corresponding frequentness N is changed into the corresponding frequency f fit the law of

$$f = \mathrm{CQ}^{-\mathrm{D}} \tag{7}$$

For NGPS, Q is the gas flow of the pipeline system, and f is the corresponding frequency of the gas flow Q. The C and D are the constants after fitting.

The gas transmission amounts are in wide range and changing differently with the order of magnitudes, for a data group of gas flow in one-year, different sections are set to measure the frequencies of corresponding gas flows. The lengths of the sections are determined by the quantitative value of the gas flow. According to Eq. (7), logarithm transformation can be applied and Eq. (7) can be transformed to

$$\ln f = C - D \ln Q \tag{8}$$

Eqs. (7) and (8) are aimed to study the characteristics of SOC.

In addition, it should be explained here that the disturbances should be understood generally, which can result in the decrease and increase. In this article, both of the two conditions are considered.

Table 9
Population and NGPS average degree of a Chinese city.

District	Location	Population density (person/km^2)	Average node degree
Fangshan	Southwest Beijing	649	5.5
Tongzhou	Southeast Beijing	2034	3.8
Daxing	South Beijing	1753	2.5
Changping	North Beijing	1687	3.5
Shunyi	Northeast Beijing	1298	2.8
Mentougou	West Beijing	273	2

2.4. R/S analysis

R/S analysis is Rescaled Range Analysis, proposed by H.E.Hurst (Hurst, 1951) and applied for the research of fractal characteristics of time series data. The fractal characteristics mean that the system is similar in whole or part in time series, and the similarity also means the

Table 10
Gas source and NGPS average degree of Ukraine.

Gas source	Location	Type of gas supply	Average node degree
BRE	Northwest	Pipeline	2
MAZ	North	Pipeline	2
BRY	North	Pipeline	3
KUR	Northeast	Pipeline	4
VOR	Northeast	Pipeline	2
BEL	Northeast	Pipeline	2

Table 11
Population and NGPS average degree of China.

Province	Location	Population density (person/km^2)	Average node degree
Hainan	South China	290	2.2
Xinjiang	Northwest China	16	2
Heilongjiang	North China	66	4
Hubei	Central China	314	2.5
Jiangsu	East China	794	2.7
Tianjin	North China	1140	4.7

Table 12
Gas source and NGPS average degree of China.

Gas source	Location	Type of gas supply	Average node degree
A	Northwest China	Pipeline	3
B	Southwest China	Pipeline	1
C	Southwest China	Pipeline	3
D	North China	Pipeline	1
E	Northeast China	LNG	1
F	South China	LNG	1

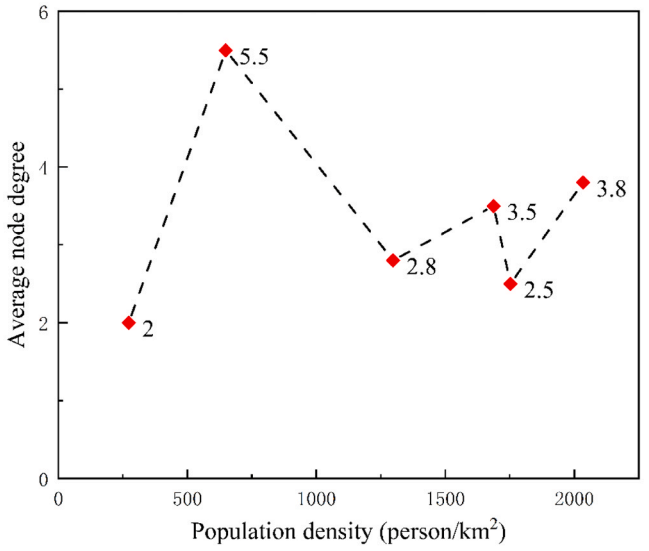

Fig. 10. Population and NGPS average degree of a Chinese city.

past changes have the effects on the future trends. The basic principle of R/S analysis is to calculate the ratio of the range (R) to the standard deviation (S) of the different sections corresponding to different time delays. If the ratio fits power-law distribution, the power exponent is Hurst exponent (H). The details of R/S analysis are:

Step 1: for the gas flows in days or few hours, the corresponding time series are $Q(t)$, $t = 1, 2, \ldots, n$, and the differences of the setting temporal granularity are

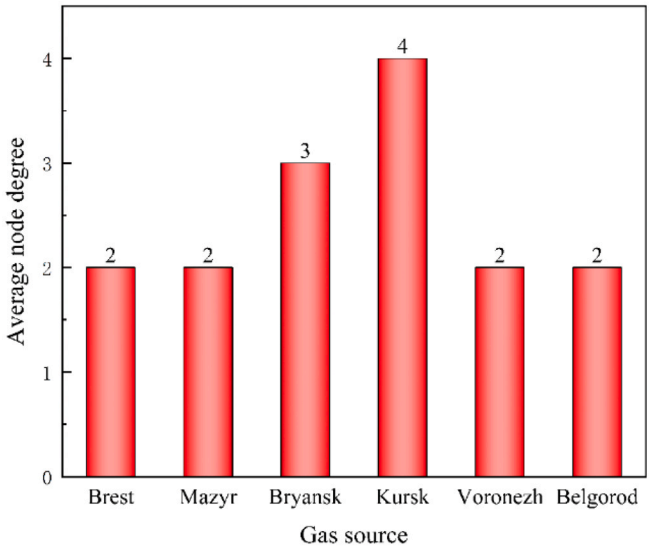

Fig. 11. Population and NGPS average degree of Ukraine.

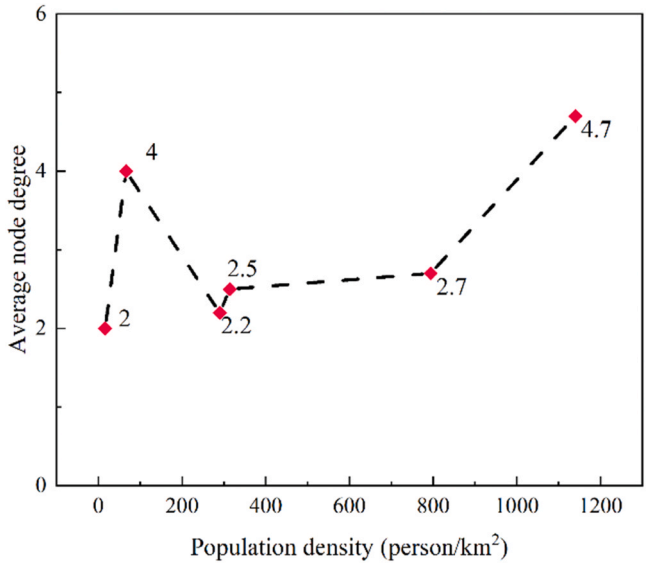

Fig. 12. Population and NGPS average degree of China.

$$\Delta Q(t) = Q(t) - Q(t-1) t = 1, 2, \cdots, n \tag{9}$$

Step 2: for different temporal range τ, the average series $\Delta Q(t)_\tau$ is calculated by Eq. (10), and the series of cumulative deviations $\Delta Q(t, \tau)$ and series of standard deviation $S(\tau)$ are

$$\Delta Q(t)_\tau = \frac{1}{\tau} \sum_{1}^{\tau} \Delta Q(t) \tau = 1, 2, \cdots, n \tag{10}$$

$$\Delta Q\left(t, \tau\right) = \sum_{1}^{\tau} \left[\Delta Q(t) - \Delta Q(t)_\tau\right] 1 \le t \le \tau \tag{11}$$

$$S(\tau) = \sqrt{\frac{1}{\tau} \sum_{1}^{\tau} \left[\Delta Q(t) - \Delta Q(t)_\tau\right]^2} \tau = 1, 2, \cdots, n \tag{12}$$

Step 3: when τ is determined, the range can be calculated by the difference between the maximum and minimum of $\Delta Q(t, \tau)$.

$$R(\tau) = \max \Delta Q(t, \tau) - \min \Delta Q(t, \tau) 1 \le t \le \tau \tag{13}$$

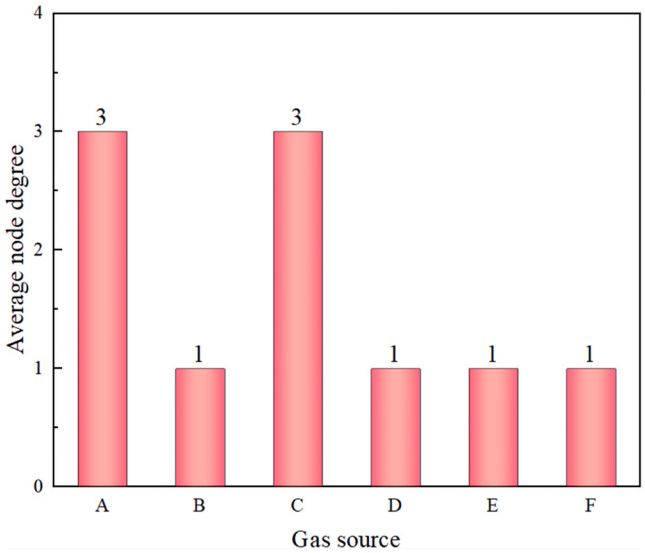

Fig. 13. Population and NGPS average degree of China.

Step 4: the ratio of range $R(\tau)$ to standard deviation $S(\tau)$ is

$$\frac{R(\tau)}{S(\tau)} = c\tau^{H} \tag{14}$$

where c is constant and H is Hurst index.

Step 5: to calculate the logarithm of Eq. (14) which is shown as

$$\ln\left(\frac{R}{S}\right) = \ln(c) + H\ln(\tau) \tag{15}$$

The minimum multiplication method is used to fit the linear relationship between ln(τ) and ln(R/S), and the slope of the fitting line is the estimation of Hurst index, which is from 0 to 1. The research methodology and logical order of this part are shown in Fig. 2.

3. Results and discussion

3.1. Atypical small world network

3.1.1. NGPS and small world network

Complex network modelling is the abstraction of a practical network into a mathematical network, which is a collection of nodes and edges, at a certain modelling expression scale. As shown in Fig. 3, three practical NGPS topologies have been applied for analysis. In this model, the connecting edges are the pipelines between the first station, the gate station and the transmission station, and the following simplifications are made: units such as regulator stations and valve chambers that do not affect the flow of the pipeline are considered as part of the pipeline and are used as edges. Since the statistical description values used are independent of the direction and weights, an undirected and unweighted graph is created, while different node types have no effect on the statistical description values and the nodes can be regarded as undifferentiated nodes.

Fig. 4. shows the comparison of degree distribution between NGPS and corresponding standard small world network. It can be concluded that the degree distributions of NGPS and the related small world networks are similar. For example, the degree distribution of NGPS case A has just shown the bell shape, which is higher in the middle and lower in the sides. The probability of average degree is higher and the nodes with average number degrees are 48% of all the nodes. With the increase of degrees, the probability decreases fast. The aggregation factor of case A is 0.12. The corresponding standard small world network is generated as the node number of 44 and the connection probability of p, which is processed by random network model. The connection probability p is calculated as the ratio of average degree to the network scale. The p of small world network is 0.07, of which the aggregation factor is 0.031. Based on the degree distribution, the NGPS has the characteristics of small world networks.

In addition, the statistical description values of the NGPS (case A as sample) were compared with a random network, a regular network and a scale-free network of the same size and two small world networks for small world network A (K=0.4 and P = 0.43) and small world network B (K=4 and P = 0.08). The results of the calculations are shown in Table 2.

From the degree distribution, it can be seen that, unlike regular networks, random networks and scale-free networks, the degree distribution of NGPS is similar to that of small world networks, which are bell-shaped distribution. Obviously, the study of the evolution mechanism of NGPS cannot refer to the evolution mechanism of regular network, random network and scale-free network. The small world network A and B take into account the randomness, and in order to attenuate the effect of randomness, the small world network is simulated and generated 1000 times respectively, and the valid interval of each statistical description value is obtained. When P = 0.08 in the WS small world model, the network is closer to the regular network, and under this condition, the average path length of NGPS is satisfying the small world model, but the aggregation factors differ significantly; when P = 0.43 in the WS small world model, the randomness of the network is enhanced, and under this condition, the aggregation coefficients of NGPS are satisfying the small world model, but the average path length is not satisfied. Although NGPS cannot be directly described by the WS small world model, the statistical description of the NGPS is very close to the WS small world model, and with atypical small world characteristics. As the statistical description of the network is a reflection of its structure, the topological characteristics of NGPS may be responsible for the differences in the statistical description values, or the reason of its atypical small world network.

3.1.2. Analysis of the structural characteristics of small world networks

In the following, small world networks with different probabilities are studied how differences in structural features affect the statistical description of small world networks. The structural information in Table 3 is obtained from simulations of the WS small world model at P = 0.08, where the sum of the 4–4, 4–5 and 3–4 structures reaches 89%, while the other structures only reach about 2%, which shows that the structural hierarchy of the network is highly differentiated. When this small world model is simulated 100 times at P = 0.08, the average path length range of the network is 4.89–6.08.

As can be seen from Table 4 more than 50% of the nodes have an aggregation coefficient up to 0.5, and the network produces a significant aggregation effect, so the overall aggregation coefficient of the network is large.

The structural information in Table 5 obtained from simulations of the WS small world model with P = 0.43. The structures of the network clearly form three sections: the first is the 3–4, 4–4 and 4–6 structures, all of which have a proportion greater than 14%; the second is the 3–6, 5–6, 3–3 and 4–5 structures, which have a proportion of around 8%; and the third is all the remaining structures, which have a proportion of around 2%. The proportion of structures within each section is very even and does not show a significant division in the structure hierarchy. The WS small world model was simulated 100 times at P = 0.43 and the percents of all 100 simulations in one structure are not beyond 18%, while the average path length of the network ranged from 3.47 to 3.61.

As can be seen from Table 6, more than 50% of the nodes have an aggregation coefficient of 0. The network does not produce a significant aggregation effect, thus reducing the overall aggregation coefficient of the network.

When comparing the two small world networks, the average path length is larger and the aggregation coefficient is relatively larger when the network structure is ‘extreme’, like small world sample A, while the

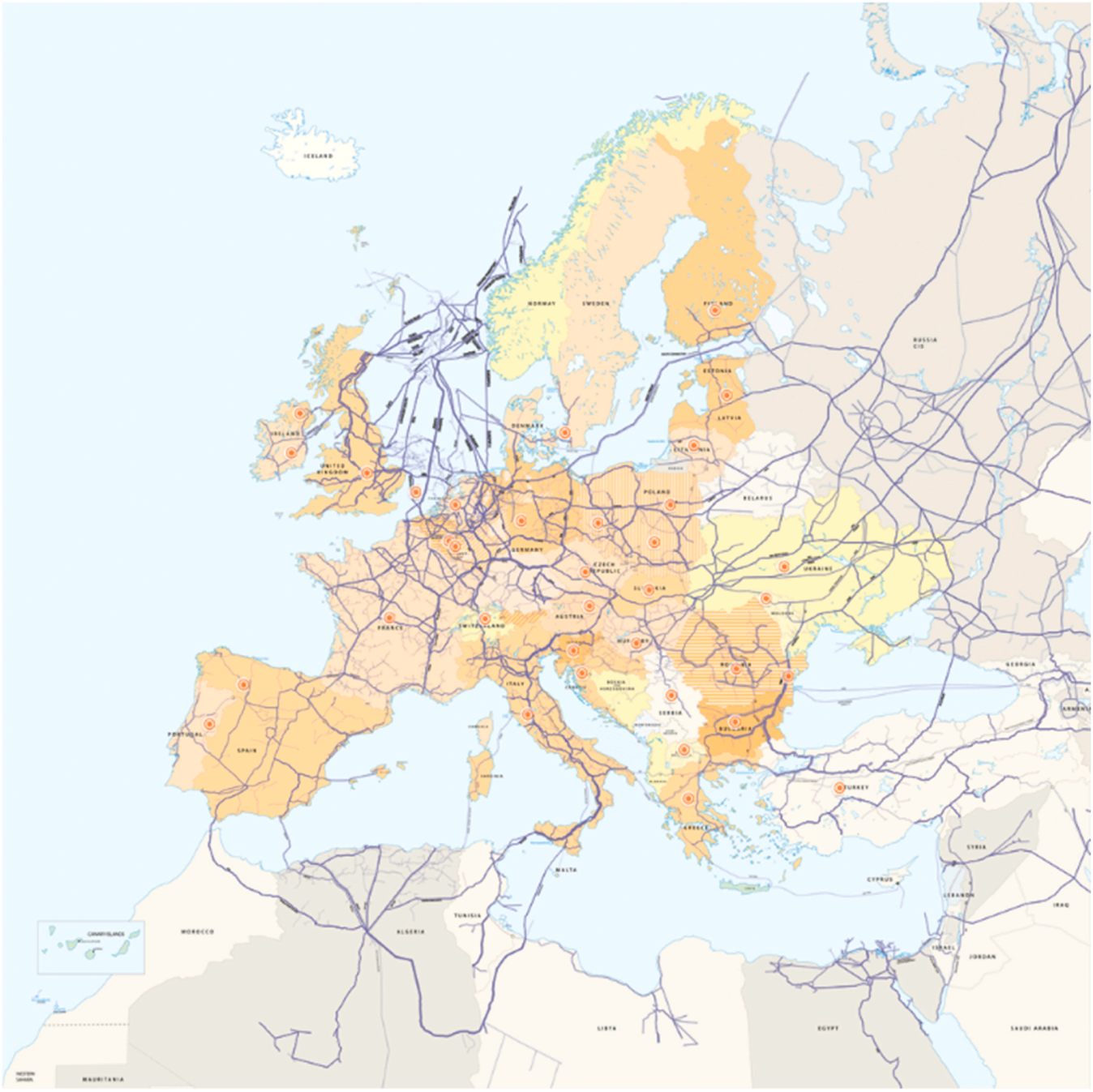

Fig. 14. Natural gas pipeline system of Europe.

average path length is shorter and the aggregation coefficient is relatively smaller when the small world network structure is hierarchical, like sample B. The above pattern is easy to explain: when the network distribution is 'extreme', the paths between nodes that are not at the centre of network have to pass through a few nodes that are at the center of 'power', thus increasing the average path length of the network. At the same time, if there is an absolute centre in the network, other nodes will naturally appear in the centre to create an aggregation effect, resulting in a high aggregation factor.

3.1.3. Analysis of the structural characteristics of NGPS

As shown in Table 7, the highest proportion of the structure of the NGPS case A is the 3–4 structure, while the proportion of each of the other structures is more average, in the range of 2% to 8%, with the 3–4 structure being the core structure of the natural gas pipeline network.

As shown in Table 8, the number of nodes with a node aggregation coefficient of 0 accounts for 74% of all network nodes, while the number of nodes with a node aggregation coefficient of 0.5 is 0, indicating that the network aggregation effect is weak.

The structure distribution of small world network A is too 'extreme', due to the high percentage of individual structures, which increases the average path between a large number of node pairs, while the network has a strong aggregation effect, which is shown in a larger aggregation coefficient and a higher average path length. The distribution of structures in small world network B is significantly hierarchical, reducing the average path between a large number of node pairs, while the aggregation effect of the network becomes weaker, which is reflected in shorter average path and smaller aggregation coefficient at the

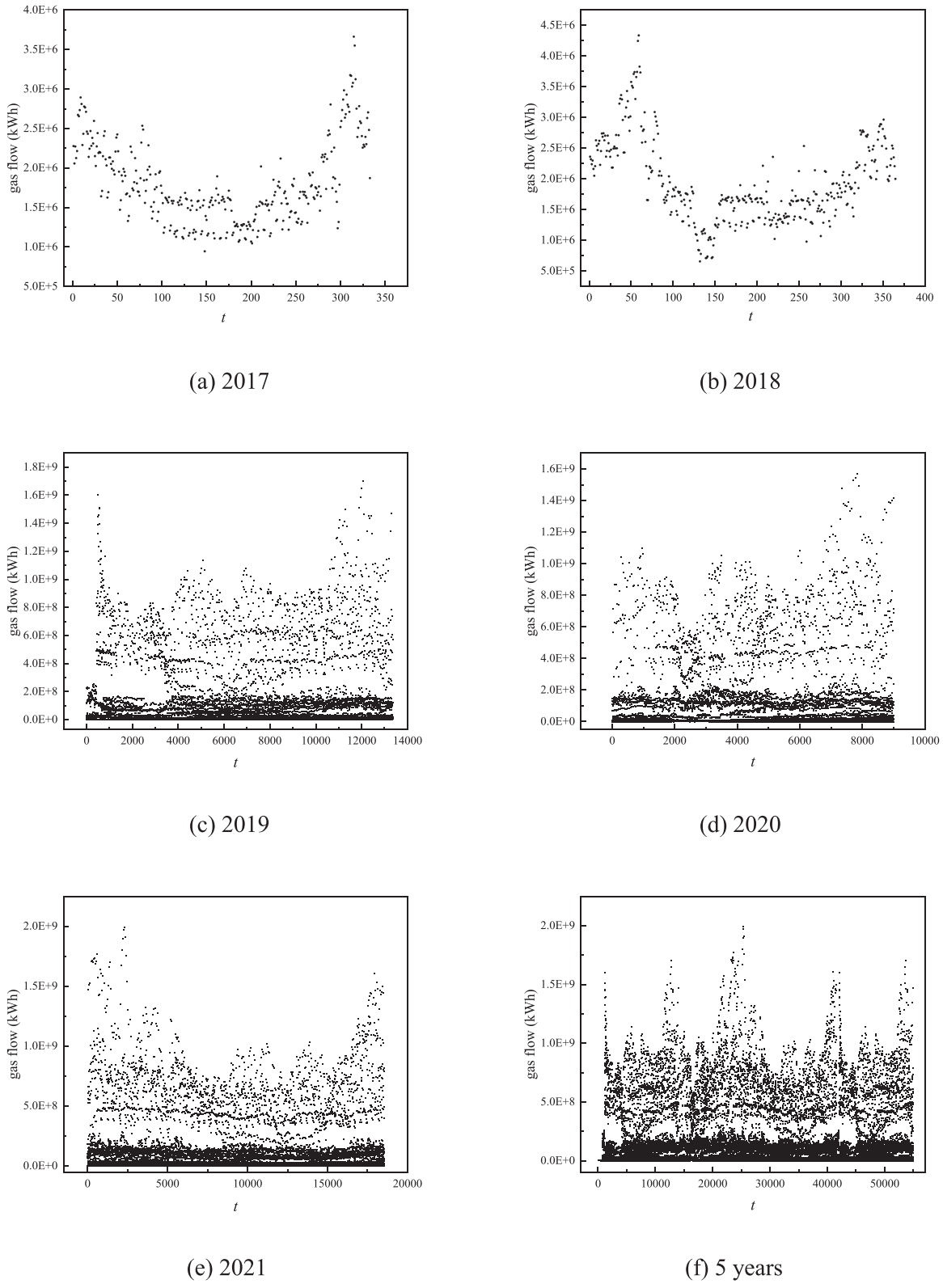

Fig. 15. Gas flow in different granularities of time.

statistical description level. Combining the above two networks characteristics, the structure of NGPS is characterized atypical small world network. On the one hand, some structures account for a much larger proportion than others, which increases the average path length of node pairs; on the other hand, the 'extreme' structure is only 22% and the other structures are more evenly distributed, thus reducing the global aggregation coefficient, which is reflected in a larger average path length and a smaller aggregation coefficient at the level of statistical description.

Through the above discussion, it can be demonstrated that the structural characteristics of NGPS lead to differences in the statistical description between NGPS and the small world network. It can be seen

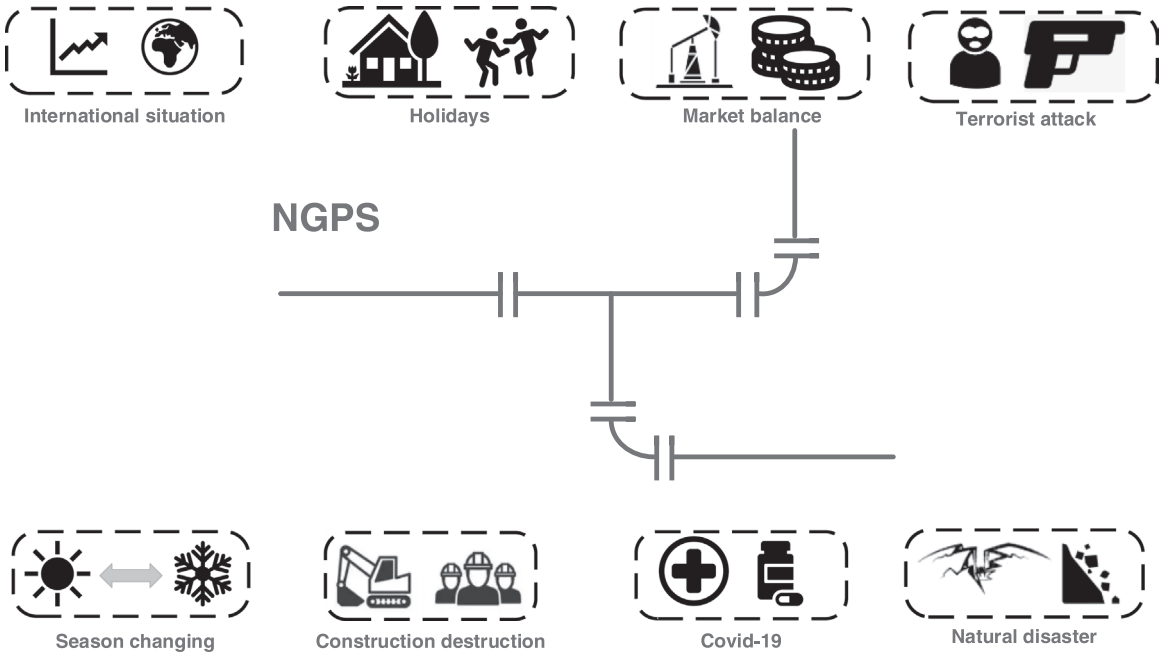

Fig. 16. Influence factors to NGPS.

that the evolutionary mechanism of the NGPS needs to be based on the evolutionary mechanism of the small world network, combined with its own structural characteristics.

3.1.4. Analysis of the evolutionary mechanism of natural gas pipeline networks

Based on observations of the topology of NGPS, this paper summarises the construction of NGPS: firstly, several gas transmission main lines are built, each of which satisfies the supply of natural gas within a certain area, and as the area and supply changes, the gas distribution lines are constructed, while different gas transmission main lines will be connected through distribution lines, thus forming an intricate and complex NGPS. The regularity of the network lies in the construction of main lines, while the connections between main lines and the distribution lines are a reflection of randomness. Further, the complexity of NGPS is closely related to its construction process.

As shown in Fig. 5, structures 3–3 and 3–4 are the two major structures of analysis of the gas pipeline network, and both structures are common to dendritic pipeline networks, so the gas transmission mainline can be, modeled as a large dendritic pipeline. The dendritic structure can be seen as the smallest spanning tree of geographic nodes, following the rule of shortest path length to connect nodes. The economics of the network is related to the total length of NGPS, so the existence of dendritic structures meets the economics requirement, which proves the rationality of the dendritic structures.

Although the dendritic structure can show the large mean path of realistic pipe networks, the low aggregation coefficient of the dendritic structure, which even reaches 0, contradicts the fact of the large aggregation coefficient of NGPS, so this paper guesses that the combined effect of economic reasons and geographical orientation causes the aggregation effect of pipe networks. Due to the influence of geographic location and low cost requirement, main lines are built to ensure the shortest distance and to adopt a proximity connection strategy. To verify this conjecture, a dynamic network model based on the proximity connection rule is developed in this paper.

The model assumes that the distance between nodes is 1. If a new node is added, the node is connected to the two nearest points. The specific model is described as follows: first, three nodes are evenly distributed around the circle, and the three nodes are connected to each other to form a complete graph, as shown in Fig. 6 (1), while the circumference is divided into three arcs of equal arc length, and the distance between each pair of nodes is 1. When a new node is added to the network, the node is randomly located in one of the three arcs and forms an edge with the two nearest nodes, as shown in Fig. 6 (2) and (3). The four nodes are then repositioned so that the four arcs formed by the four nodes are of equal length, and the above steps are repeated after a new node is subsequently added.

Simulation experiments were carried out on the model and Fig. 7 shows a network with 50 nodes, and 100 nodes.

In this paper, networks with different numbers of nodes are obtained through model simulation, and the corresponding network aggregation coefficients and average path lengths of different networks are counted separately.

As shown in Fig. 8, the aggregation coefficients of several simulated networks are distributed around 0.65. When the number of nodes of the network is 100, the global aggregation coefficient of the network is 0.6495; when the size of the network increases to 100000, the global aggregation coefficient of the network is 0.6421, the size of the network increases by a factor of 1000, but the change of the aggregation coefficient is very small. Compared to a random network of the same size, the global aggregation coefficients of the other kind of networks are large in all an order of magnitude.

As shown in Fig. 9, although the number of nodes grows exponentially, the average path length of the network does not change by the same magnitude, and the rate of change in the average path length continues to decrease as the number of nodes increases.

The above simulation results show that the dynamic network model based on the proximity connection rule has a large aggregation factor and the average path length does not change much with increasing size, thus the network formed by this model has small world characteristics, thus verifying the conjecture of this paper that the pipe network adopts a proximity connection strategy due to economical reasons and geographical location, and the proximity connection strategy can bring about an aggregation effect.

The above analysis shows that, after comparisons with the basic networks, the NGPS is basically close to the small world network, but the structural characteristics itself cause differences between the typical small world networks. The dendritic structure of the network increases

Table 13
Statistics of section and frequency of yearly gas flows.

Time	Section medium (kWh)	Count	Frequency
2017	1.05E+ 06	33	0.0991
	1.35E+ 06	63	0.18919
	1.65E+ 06	108	0.32432
	1.95E+ 06	38	0.11411
	2.25E+ 06	41	0.12312
	2.55E+ 06	26	0.07808
	2.85E+ 06	17	0.05105
	3.15E+ 06	5	0.01502
	3.45E+ 06	1	0.003
	3.75E+ 06	1	0.003
2018	8.00E+ 05	12	0.03288
	1.20E+ 06	72	0.19726
	1.60E+ 06	115	0.31507
	2.00E+ 06	56	0.15342
	2.40E+ 06	48	0.13151
	2.80E+ 06	38	0.10411
	3.20E+ 06	12	0.03288
	3.60E+ 06	9	0.02466
	4.00E+ 06	1	0.00274
	4.40E+ 06	2	0.00548
2019	0	2306	0.172695
	5.00E+ 05	686	0.051374
	5.00E+ 06	2828	0.211787
	5.00E+ 07	5932	0.444244
	2.70E+ 08	285	0.02134
	4.50E+ 08	431	0.03228
	6.30E+ 08	427	0.03198
	8.10E+ 08	278	0.02082
	9.90E+ 08	118	0.00884
	1.17E+ 09	29	0.00217
	1.35E+ 09	17	0.00127
	1.53E+ 09	12	8.99E-04
	1.71E+ 09	2	1.50E-04
2020	0	817	0.09079
	8.00E+ 06	3563	0.39597
	5.00E+ 07	1534	0.17048
	5.00E+ 08	2281	0.2535
	6.3E+ 08	286	0.03178
	8.1E+ 08	211	0.02345
	9.9E+ 08	94	0.01045
	1.17E+ 09	18	0.002
	1.35E+ 09	15	0.00167
	1.53E+ 09	5	0.000556
	1.71E+ 09	0	0
2021	0	2160	0.11648
	5.00E+ 05	1385	0.074688
	5.00E+ 06	3453	0.186207
	5.00E+ 07	7257	0.391341
	1.00E+ 08	2165	0.11675
	3.00E+ 08	458	0.0247
	5.00E+ 08	722	0.03893
	7.00E+ 08	543	0.02928
	9.00E+ 08	228	0.0123
	1.10E+ 09	101	0.00545
	1.30E+ 09	27	0.00146
	1.50E+ 09	24	0.00129
	1.70E+ 09	15	8.09E-04
	1.90E+ 09	5	2.70E-04
Five years	0	6739	0.122648
	5.00E+ 05	3969	0.072234
	5.00E+ 06	11949	0.217468
	5.00E+ 07	18924	0.34441
	1.00E+ 08	6871	0.12505
	3.00E+ 08	1414	0.02573
	5.00E+ 08	2165	0.0394
	7.00E+ 08	1635	0.02976
	9.00E+ 08	852	0.01551
	1.10E+ 09	268	0.00488
	1.30E+ 09	75	0.00136
	1.50E+ 09	59	0.00107
	1.70E+ 09	21	3.82E-04
	1.90E+ 09	5	9.10E-05

the average path length of the network as a whole, which also has a low aggregation effect. However, the NGPS construction is influenced by a combination of economic and geographical factors, which can offset the low aggregation effect of the dendritic network structure. The combined effect of these factors causes that NGPS is atypical small world network, but with a larger mean path than a standard small world network, and an aggregation factor close to that of a standard small world network.

3.1.5. Analysis of other effects on the NGPS topology

Small-world networks are characterized by the presence of highly interconnected clusters or communities of nodes and relatively short, efficient paths between these clusters, which enables the rapid transfer of information or interactions across the network. Based on the analysis of atypical small world above, there are also some geographic, topological, environmental and other factors affecting NGPS layout, such as the location of gas sources, population centers, and geographic features. Three different NGPS models in different scales, which are from China, Ukraine, and a city of China. The nodes degrees are selected to represent NGPS layout. The degrees of different gas sources and populations are shown in Tables 9–12 and Figs. 10–13.

Based on the results, the gas sources and populations from different geographic areas have different effects on the NGPS topology. It seems to be different from what we thought. The node degrees are not positively related to population. The degrees are not dependent on whether the nodes are near gas sources. In reality, the NGPS layout is dependent on many factors, such as geographic condition, local policy, NGPS design and other social factors. For NGPS in different scales, the effects of population and gas source are related to NGPS function, scale and practical environment condition. For example, the NGPS in country level is main line system with high pressure and large size, the function of which is transporting gas through long distance. However, the NGPS in city level is with lower pressure and smaller size, transporting gas through shorter distance. The average degree of country level is lower than city level, but the latter is affected more that the former. The function of NGPS can also affect the layout. The NGPS of China is mainly aimed to import gas and distribute to the provinces and cities, but that of Russia needs to care more about output gas to other countries.

In reality, it is important but difficult to analyze the environmental effects on the NGPS topology. However, the topology of NGPS is also the result of all the factors including population, gas source and geographic features, which contributes to the atypical small world characteristics of NGPS.

3.2. Atypical Self-organized Criticality

3.2.1. Characteristics of NGPS flow data

The operation data of NGPS are based on practical NGPS daily logs of 2017–2021 from Europe (Entsog, 2021), because of the data integrity and transparency. The NGPS of Europe is shown in Fig. 14. The gas flows in NGPS with different granularities of time are chosen as the objective data groups as shown in Fig. 15. The general tendency of the annular gas flow shows the maximums are in the beginning and end of each year, and smaller in the middle period. This is related to the temperature of the year, which results in the gas demand differences. There are the order of magnitudes, because the data of 2017 and 2018 gas flow are focused on the part area of Europe, and the data of 2019–2021 are focused on the Europe-wide scale. For granularities of time, the data of 2017 and 2018 are in days of the whole year, and the data of 2019–2021 are in the 1–3 h as the sampling periods. The gas flow in NGPS can be a reflection of the degree of normal operation. There are two types of disturbances for NGPS in which the gas flow can change significantly. The disturbance such as natural disasters, deliberately sabotage, accident destroy et al., can make the pipes or stations destroyed, which lead to the decrease of the gas flow in NGPS. The other disturbance like seasons changing, general holidays, and even Covid-19 which resulted in people staying at home, can lead to the increase of the gas flow in

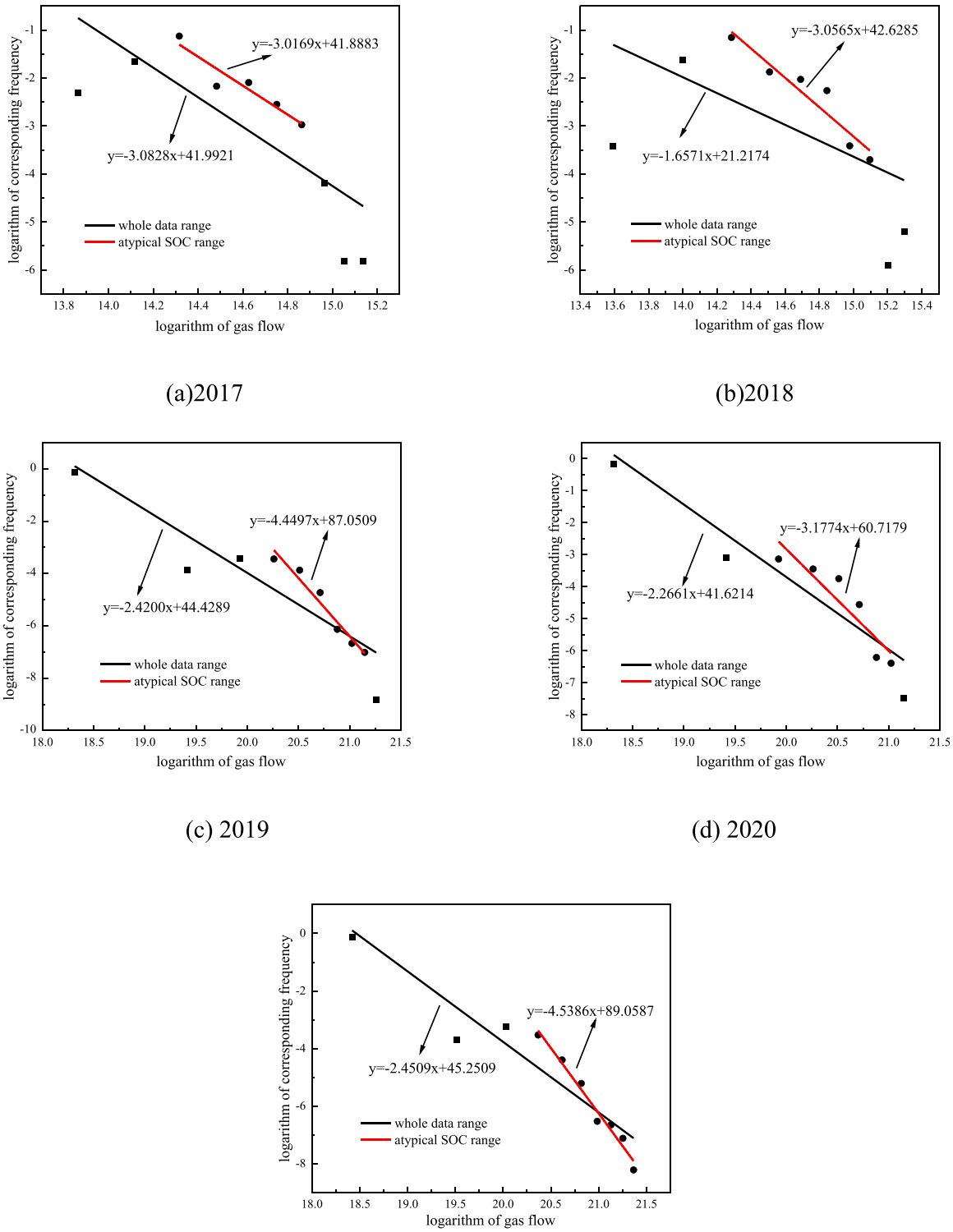

Fig. 17. Power law of logarithm of gas flow and corresponding frequency.

NGPS. The kinds of disturbance can be seen in Fig. 16.

It can be concluded that the majority of gas flow in each year has the corresponding range of gas transmission amount or the corresponding order of magnitudes. Fig. 15(a)-(f) shows the gas flow for five years, for example, the most of data points can be seen in the bottom of the figures. The details of the data points distribution and the corresponding frequencies are shown in Table 13. In 2017 and 2018, the majority of the gas flow are focused on $1.3–2.0 \times 10^6$ kWh, which contribute to 60–65% of all the samplings. In 2019–2021, most data points are in the orders of magnitudes within 10^6 and 10^7. The gas flow data show that NGPS keeps operating in stable status. This is because the gas flow depends on the interaction of the supply and demand sides, which is

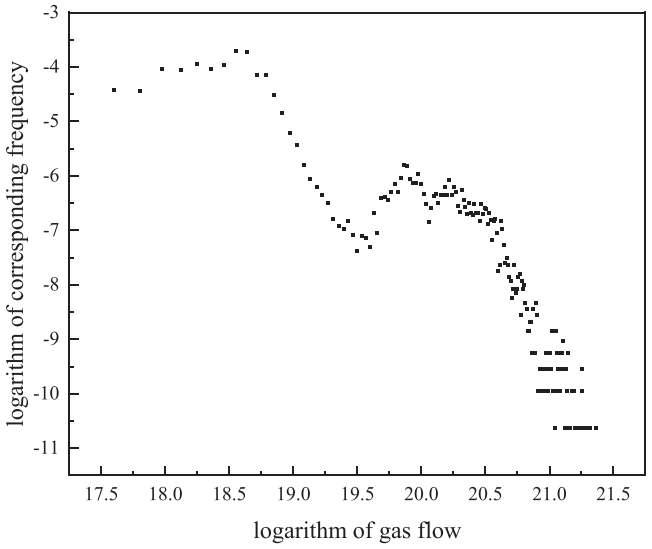

Fig. 18. Logarithm of gas flow and corresponding frequency for five years.

Table 14
Parameters of whole range fitting lines in different years.

Data group	b	K	R^2
2017	41.9921	-3.0828	0.6116
2018	21.2174	-1.6571	0.3433
2019	44.4289	-2.4200	0.8273
2020	41.6214	-2.2661	0.8697
2021	45.2509	-2.4509	0.8927
section 18.63579–19.5649	71.1669	-4.0237	0.9717
section 19.86524–21.1511	66.3992	-3.6000	0.8506

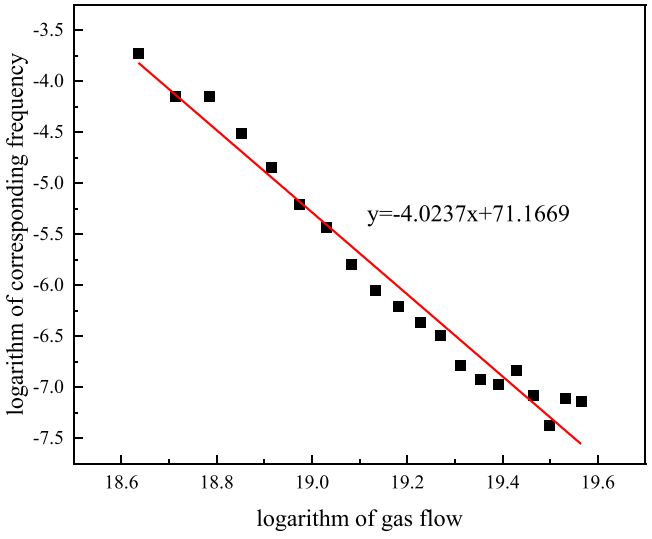

Fig. 19. Logarithm of gas flow and corresponding frequency in linear range.

reflected in the gas company daily logs. From a macro perspective, the overall supply and demand do not have a sudden increase and decrease, especially for the scope of whole Europe. Except the international large-scale regional conflicts, the overall condition is relatively stable.

Different from power grids networks, the stable range is at the fewer amount level of the whole data group. The reason for that is the kinds of disturbances described above. Most of the pipes of NGPS are buried underground, and the importance of NGPS for countries and people

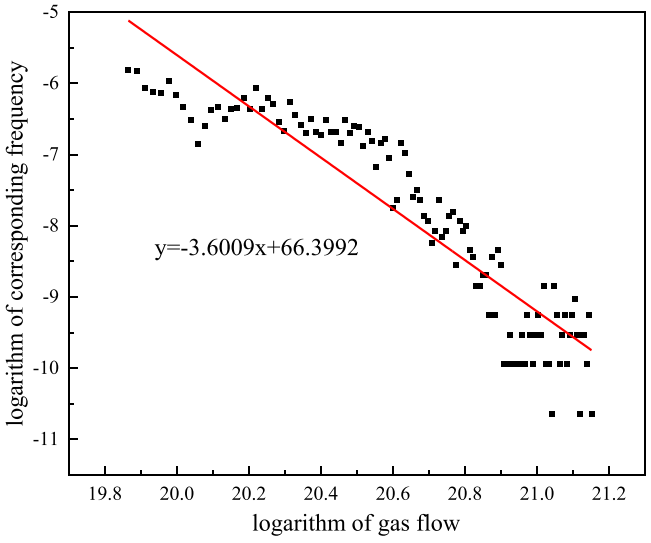

Fig. 20. Logarithm of gas flow and corresponding frequency in linear range.

Table 15
Parameters of the linear range fitting lines in different years.

Year	b	k	R^2
2017	41.8883	-3.0169	0.8997
2018	42.6285	-3.0565	0.9072
2019	87.0509	-4.4497	0.9564
2020	60.7179	-3.1774	0.8429
2021	89.0587	-4.5386	0.9745

living make the pipes protected well. As a result, the disturbance such as natural disasters, deliberately sabotage, accident destroy et al., which lead to the decrease of the gas flow in NGPS, can be forbidden in a certain extent and the events of gas flow decrease become smaller probability events. In other words, most of the disturbances which can results in the increase of gas flow in NGPS, are usually regular and predictable, and they also happened easily and in more times.

In reality, the data for SOC analysis are usually using the loss of system function and the corresponding frequencies, however, the kinds of data which can reflect the NGPS loss and failure, such as the amount of natural gas leakage, or the amount of the gas shortage due to the disturbances, are few to be found. The gas flow in NGPS of Europe are applied for the SOC analysis based on the corresponding frequencies are counted.

3.2.2. *Power law analysis*

The gas flow of European NGPS, together with the corresponding frequencies, from 2017 to 2021 are collected and in logarithmic transformation, as shown in Fig. 17 and Fig. 18. For the gas flow in each year, all the data groups are divided into subintervals based on the range of data. The x-axis has been marked by the median of each section after logarithmic transformation, and the y-axis is the number of the corresponding gas flow section after logarithmic transformation. Table 14 shows the slope and intercept of the fitting function of gas flow and frequency in logarithmic transformation in five years, together with the Goodness of Fit, R^2, which is used as the index to measure the linear properties of the logarithmic gas flow and its frequency. The calculation of R^2 is

$$R^2 = \frac{S_{YY} - SS_R}{S_{YY}} = 1 - \frac{SS_R}{S_{YY}} \tag{16}$$

where the S_{YY} and SS_R are

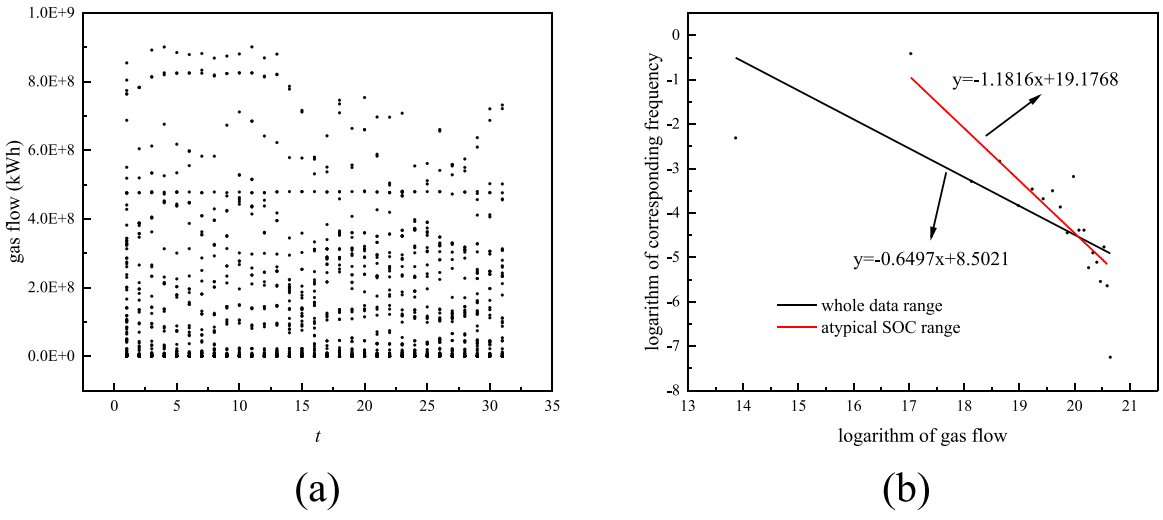

Fig. 21. Gas transportation data of Belgium NGPS in January.

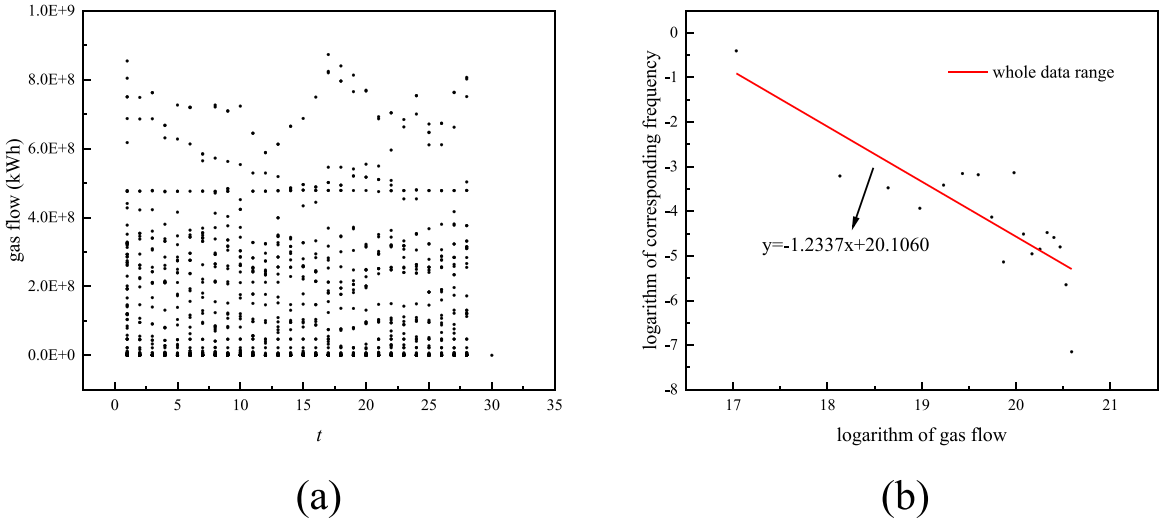

Fig. 22. Gas transportation data of Belgium NGPS in February.

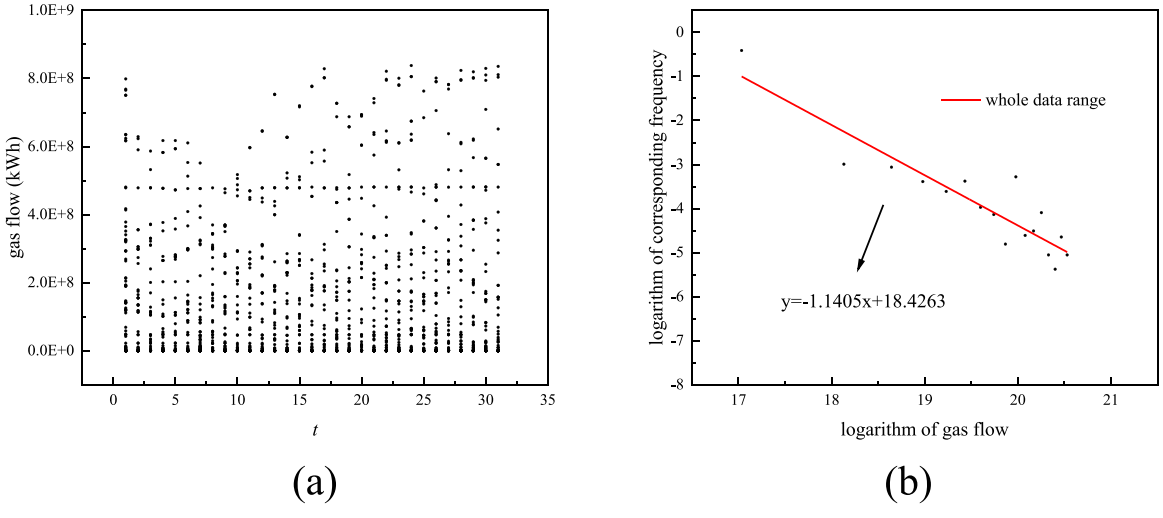

Fig. 23. Gas transportation data of Belgium NGPS in March.

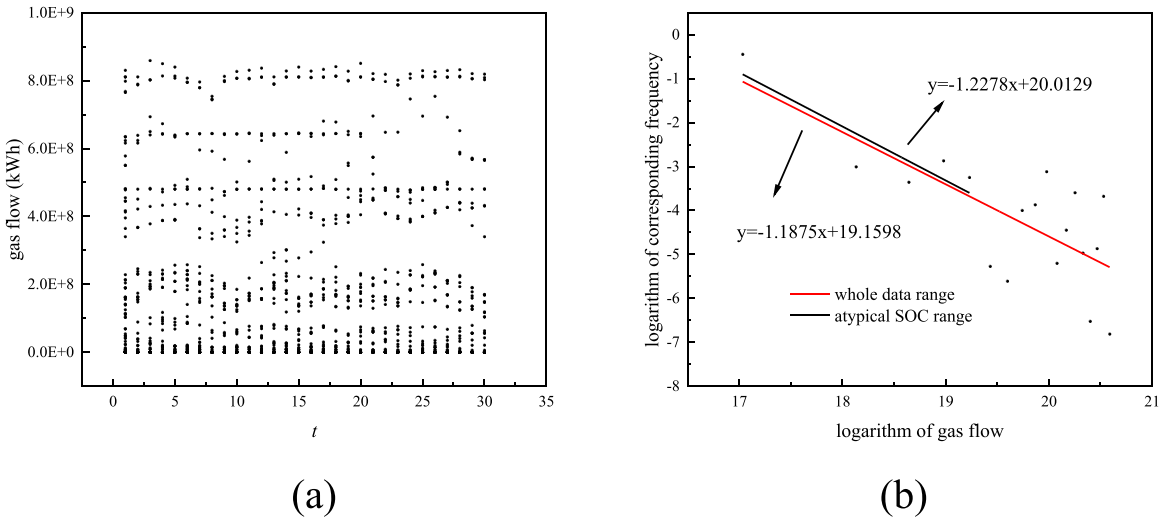

Fig. 24. Gas transportation data of Belgium NGPS in April.

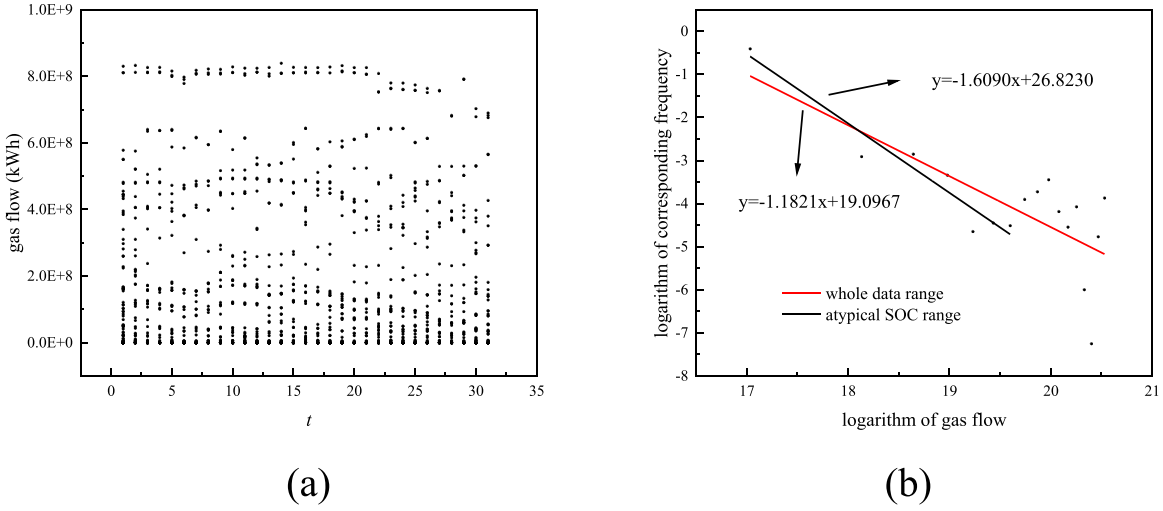

Fig. 25. Gas transportation data of Belgium NGPS in May.

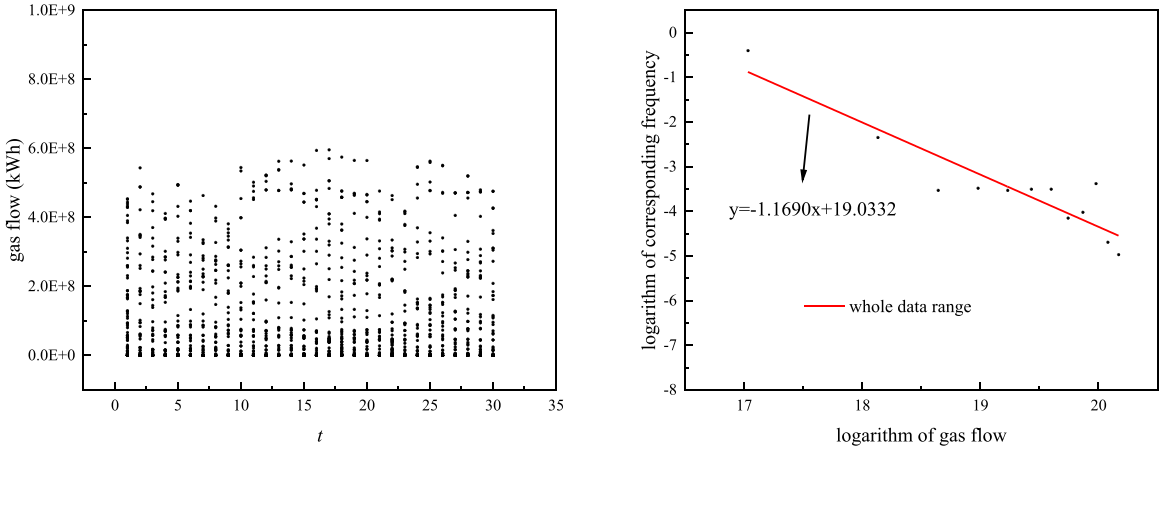

Fig. 26. Gas transportation data of Belgium NGPS in June.

Table 16
Parameters of whole range fitting lines in different periods.

Data group	b	K	R^2
January	8.5021	-0.6497	0.5236
February	20.1060	-1.2337	0.6972
March	18.4263	-1.1405	0.8437
April	19.1598	-1.1875	0.5584
May	19.0967	-1.1821	0.6087
June	19.0332	-1.1690	0.848

Table 17
Parameters of linear range fitting lines in different periods.

Data group	b	K	R^2
January	19.1768	-1.1816	0.8212
February	20.1060	-1.2337	0.6972
March	18.4263	-1.1405	0.8437
April	20.0129	-1.2278	0.7766
May	26.8230	-1.6090	0.932
June	19.0332	-1.1690	0.848

$$S_{YY} = \sum_{i=1}^{n} (Y_i - \overline{Y})^2 \tag{17}$$

$$SS_R = \sum_{i=1}^{n} (Y_i - A - Bx_i)^2 \tag{18}$$

To combine the variables of NGPS SOC analysis with Eqs. (1) and (2), the power law relationship has been changed to

$$\ln f = C - D \ln Q \tag{19}$$

where f is the corresponding gas flow frequency, and Q is the transformed gas flow in NGPS, kWh.

It can be seen from Fig. 17 that the NGPS has shown weak linear correlation between logarithm of gas flow and that of the frequency, where only part of the data set fits the linear relation. For the data of each year, the different geographic scopes have different SOC characteristics. The NGPS of the whole Europe has the better SOC property than that of the part area. The reason for that is that the extreme condition is more easily to happen in the part area than the whole Europe, and the part area can amplify the effects of disturbance. In addition, the extreme conditions of NGPS are in the frequency with fewer orders of magnitudes than others. The reasons for that are: 1) the line-pack of NGPS results in time lags in the pipelines, which is different from the power grids system, and the time lags can support more time for the staff to deal with kinds of disturbances, so that the large cascade failure can be prevented effectively. 2) the policies and importance of NGPS require safety overmeasure for the NGPS, and the characteristics of the disturbances, which can affect the gas flow, determine the lower frequency of the extreme conditions. Based on this characteristic of NGPS, it shows the atypical SOC properties, which means the gas flows have SOC among the special section, where the red fitting line covers. The NGPS has SOC property under a specific flow range, which already includes the flow under extreme events in daily production, while for more extreme events, the law of SOC is escaped.

The extreme events or extreme gas flow can be classified into two kinds. One kind is the gas flow still in the SOC range including disturbance happening frequency, and the other kind is the gas flow and the corresponding frequency are without the power law range. For the SOC extreme disturbance, that means this kind of disturbance has the frequency in the power law, and the finding of SOC range in NGPS can guide the guard against all kinds of events and help the knowledge of the law of disturbance events happening. In addition, 1) for the events whose happening frequency and the gas flow fit the power law, the reasons of those are usually predicted and regular, such as seasons changing or other temporal festivals. This kind of extreme events can be controlled by the SCADA system or the gas storage, line-pack etc., which bring the time lags to the gas company when the disturbance happens. As described above, the political status and the importance of NGPS make the gas storage methods such as gas storage tanks, LNG storage, line-pack and other methods to ensure the gas supply and to enhance the NGPS resilience. 2) For the extreme events of which the happening frequency are without the SOC range, they usually happen with much lower frequency than those within the range. Since they are not in the range, those types of disturbances are difficult to predict or prevent. The reasons for the lower frequency are that firstly, most of the pipes are buried underground, in order to prevent the pipes from being physically attacked; secondly, the important status of NGPS pushes the related control and monitor system developed, such as SCADA and internal inspection technologies; thirdly, the compressible properties of natural gas result in the line-pack of NGPS, so as to prevent cascade effects like the power grid system. However, such disturbance can not be ignored, and the disturbance should be focused without classifying their types.

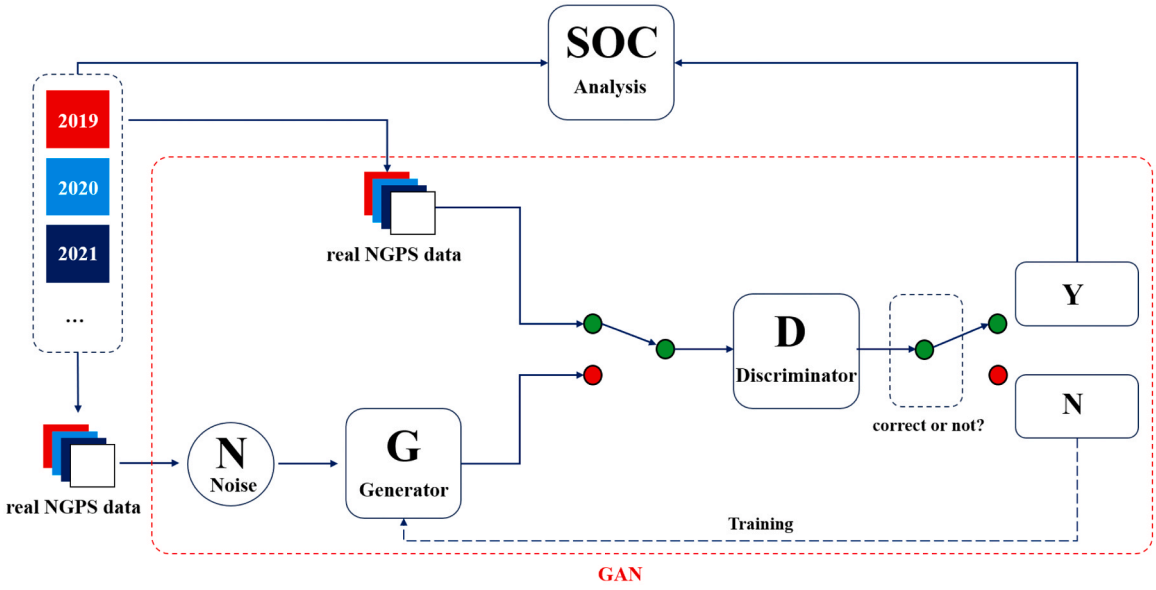

Fig. 27. Data flow of SOC analysis combined with GAN.

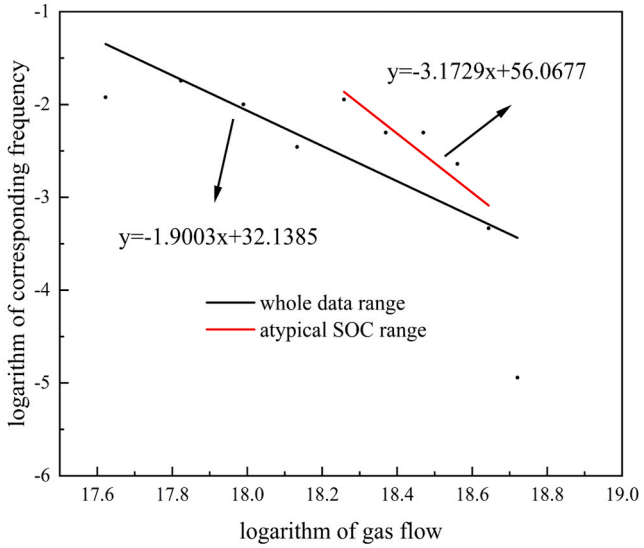

Fig. 28. Data group A enhanced by GAN.

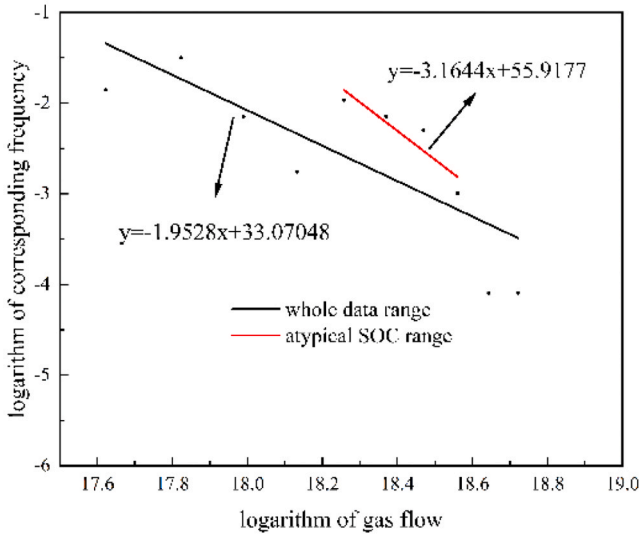

Fig. 29. Data group B enhanced by GAN.

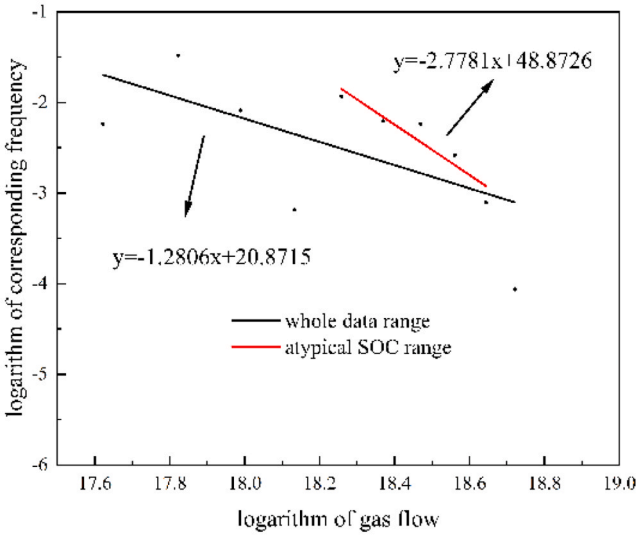

Fig. 30. Data group C enhanced by GAN.

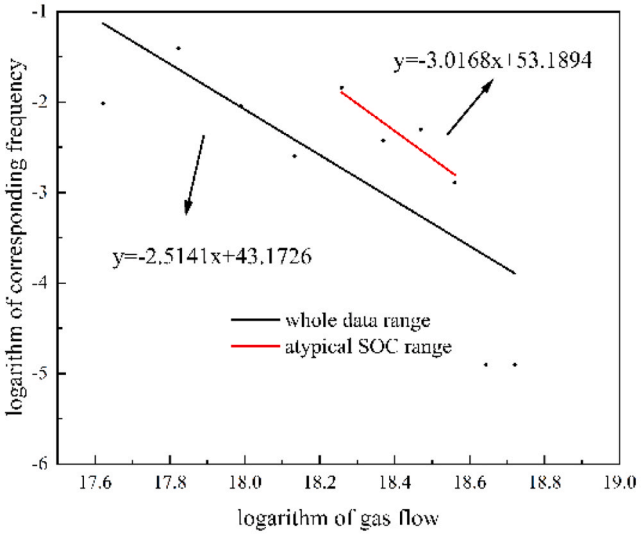

Fig. 31. Data group D enhanced by GAN.

For the five years data, it can be seen from Fig. 18 that there are two data sections which fit the SOC property roughly, and the logarithm ranges are 18.5–19.5 and 20–21.5. Fig. 19 and Fig. 20 are the relations of the two linear ranges. Table 14 and Table 15 show the details of the parameters of the fitting line, including k, b and R^2. Table 10 is for the whole data group, including the special data range in Fig. 15 and Fig. 16, and Table 11 is for the relative SOC data group. Two factors contribute to the degree of coincidence of the power law among the frequency and gas flow after logarithm transformation. One is the dataset itself, which depends on the quantity and quality of data. Another is the range of data, which depends on the scale of NGPS, because NGPS is proved that it has SOC characteristics in the special range of gas flow.

3.2.3. *Data enhancement and theoretical verification*

In order to make sure the theory consistent across different datasets, other data are added to verify the atypical SOC characteristics of NGPS. The data expansion has been applied in two methods, which are new country's NGPS data in different scale, and data enhancement. Besides the whole and part of Europe NGPS transportation data, the corresponding data of Belgium in 2023 has been applied, which are shown in Figs. 21–26, and the data source is ENTSOG.

The details of the SOC analysis results from the same method are shown in Tables 16 and 17. Based on the results, except those in February and March, the NGPS transportation data of Belgium also show the power law fitting partial range. However, the data in February, March and June have good linear relationship over the whole range. The analysis of NGPS data of Belgium proves the atypical SOC characteristics furtherly.

In addition, since the practical data are limited to be used and analyzed, data science has been applied to enhance the data group. Generative adversarial network (GAN), which performs better in data enhancement than other machine learning algorithms, is chosen to be used in data expansion. The whole data analysis framework is shown in Fig. 27. For the enhanced data, the results of SOC analysis are shown in Figs. 28–32 and Tables 18–19. The data groups from GAN have better linear relation in part of gas flow values than the whole range. Compared with other analysis, the data enhanced by GAN also show similar characteristics with other data, which verify atypical SOC of NGPS.

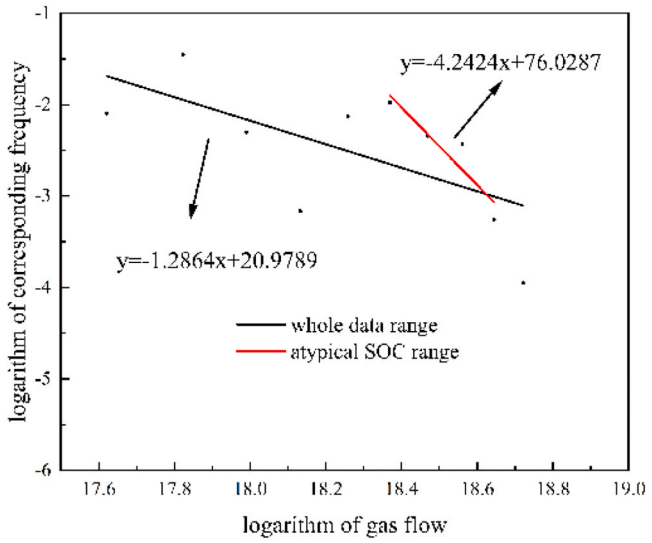

Fig. 32. Data group F enhanced by GAN.

Table 18
Parameters of whole range fitting lines in different periods.

Data group	*b*	*K*	R^2
A	32.1385	-1.9003	0.5259
B	33.0704	-1.9528	0.6221
C	20.8715	-1.2806	0.3884
D	43.1726	-2.5141	0.5666
E	20.9789	-1.2864	0.40539

Table 19
Parameters of linear range fitting lines in different periods.

Data group	*b*	*K*	R^2
A	56.0677	-3.1729	0.8527
B	55.9177	-3.1644	0.8376
C	48.8726	-2.7781	0.8828
D	53.1894	-3.0168	0.8235
E	76.0287	-4.2424	0.8575

3.2.4. Robustness test

For NGPS SOC analysis, there are two kinds of changes. One kind is the practical change which is caused by the disturbances, such as natural disasters, operation disturbances and gas market fluctuation. Since the historical data are used to study SOC characteristics, it is hard to make or simulate the practical changes directly to the NGPS. In addition, the historical data are the results of combined disturbances. The other kind of changes are data changes, such as fluctuations and noise added to the data. The fluctuation and noise can simulate the disturbances effects, which are available and convenient for us. Because the order of magnitudes is large, a wide range of noise for the historical data has been set.

Based on the atypical SOC characteristics analysis and verification, the robustness test is conducted by combining Gaussian noise and practical data. The European gas flow data in 2019 is chosen to be added noise and the results of SOC analysis are shown in Figs. 33–35.

As shown in Figs. 33–35 and Tables 20 and 21, the atypical SOC characteristics are also suitable for the fluctuant data with noise. The robustness tests have been conducted with a wide range of Gaussian noise. The standard deviation of noise has been set in order of magnitudes from 10–10^7. Based on the data enhancement and robustness tests, the atypical SOC theory can be proved better.

In conclusion, the changes caused by practical disturbances are complex and difficult to analyze. It is convenient to use noise to simulate fluctuation and changes without considering disturbances types. The results based on the SOC characteristics analysis with noise prove that NGPS is steady when meeting with changes, and such atypical SOC characteristics are suitable for NGPS with external factors.

3.2.5. R/S analysis of NGPS

When a system is analyzed based on the SOC characteristics, the R/S characteristics are usually analyzed after that. The Hurst index is between 0–1 and its value can be divided into three ranges. The first range of H is $0.5 < H < 1$, which means future trend are positively correlated with past conditions. The increase in the past can mean the future increase, also the same as decrease. The closer is to 1, the stronger dependency of the data has. Secondly, if $0 < H < 0.5$, that means future trend are negatively correlated with past conditions in the long run. The increase in the past can result in the future decrease, also adverse to the decrease. The closer is to 0, the weaker dependency of the data has. Thirdly, if $H = 0.5$, that means the data in the past and future are independent and uncorrelated with each other, and the process is random.

The results from R/S analysis are shown in Fig. 36. and the H are shown in Table 22. The R/S properties of NGPS depend on the temporal granularity, for the data with finer granularity, such as the later three years, have better Hurst properties. That means the history condition has

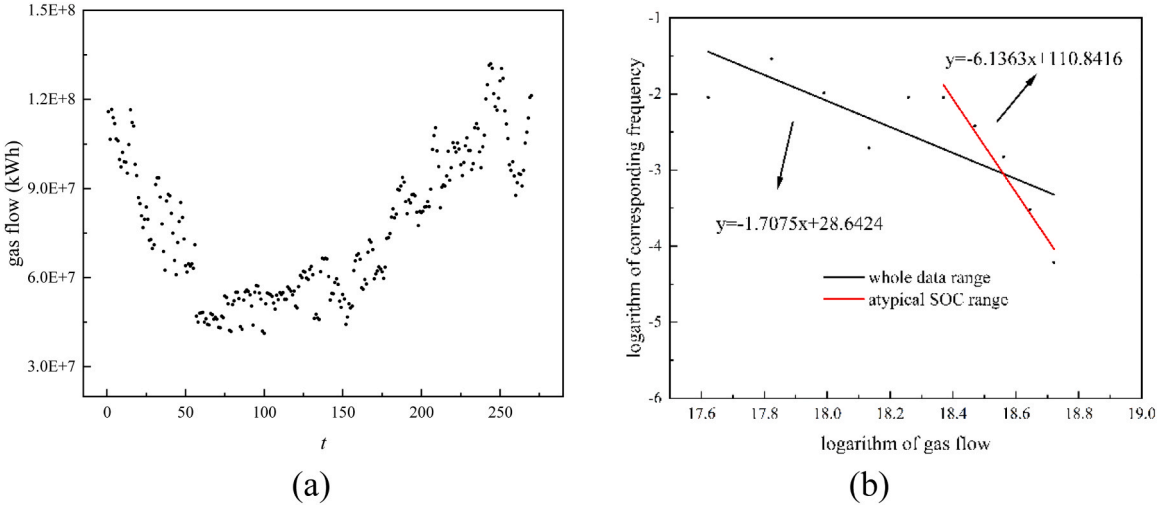

Fig. 33. Gas transportation data of Europe NGPS in 2019 with noise A.

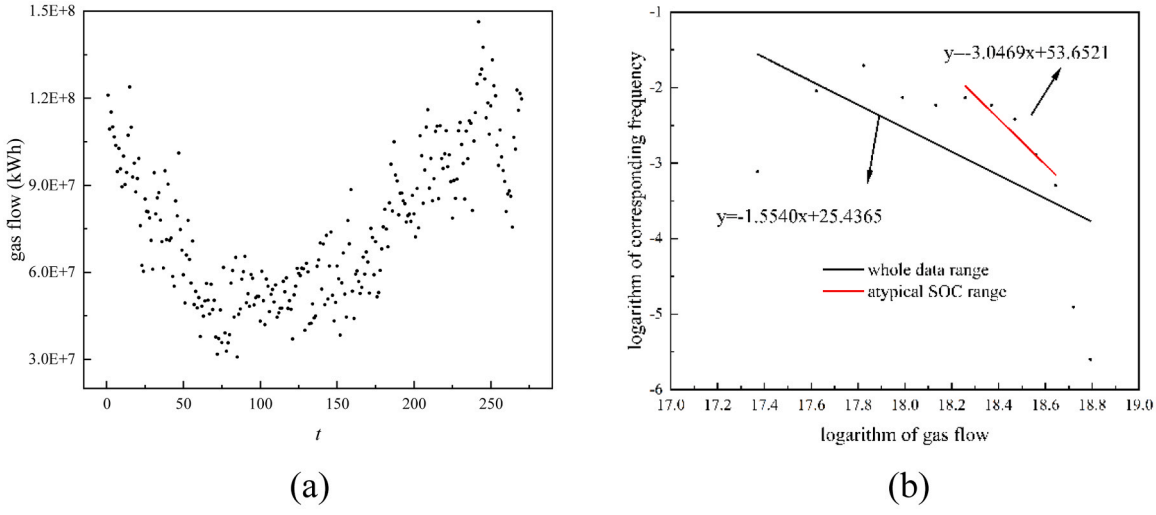

Fig. 34. Gas transportation data of Europe NGPS in 2019 with noise B.

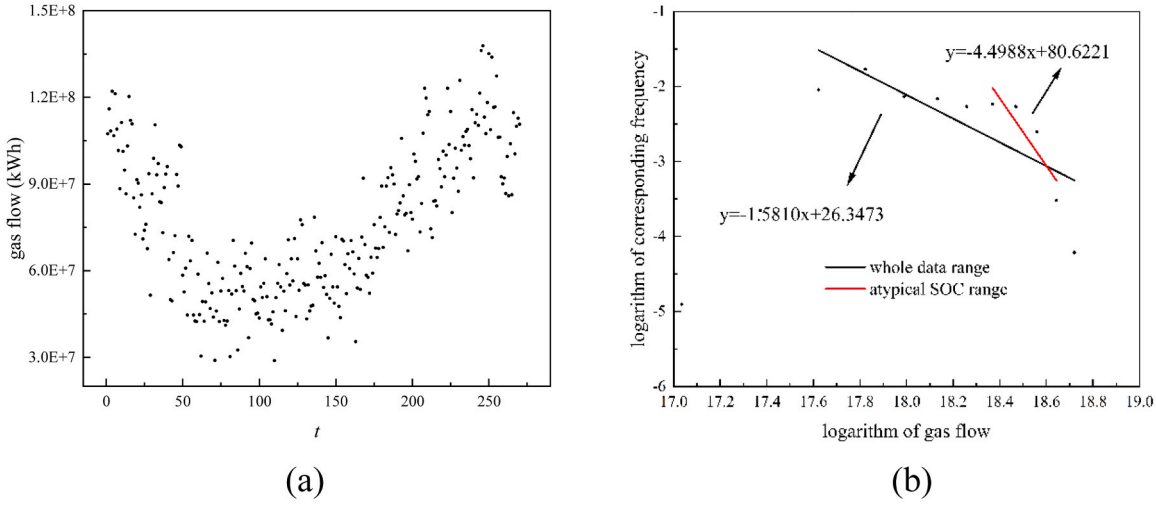

Fig. 35. Gas transportation data of Europe NGPS in 2019 with noise C.

Table 20
Parameters of whole range fitting lines in different periods.

Noise type	Noise standard deviation	b	K	R^2
A	2×10^1-3×10^2	28.6424	-1.7075	0.5865
B	8×10^6	25.4365	-1.5540	0.5792
C	1×10^7	26.3473	-1.5810	0.3411

Table 21
Parameters of linear range fitting lines in different periods.

Noise type	Noise standard deviation	b	K	R^2
A	2×10^1-3×10^2	110.8416	-6.1363	0.9615
B	8×10^6	53.6521	-3.0469	0.7846
C	1×10^7	80.6221	-4.4988	0.9033

stronger effects on the future data than the first two years. However, the H in 2019–2021 are close to 0.5, based on the reality of NGPS, the gas flow data in hours are independent, which means in a single year, the hourly gas flow in the past has weak correlation with the future gas flow. For the daily gas flow, H are from 0 to 0.5, and the negative correlation in 2017 is stronger than that in 2018. The reason for that is the extremums of 2018 are closer to the beginning and ending of the year which is more like V shape, but the trend in 2017 is not a pure V shape, more like a part of W shape. Based on the results of SOC analysis and R/S analysis, it is proved that the effects of sudden accident are independent and NGPS is absent from the cascade failures like power grid system. For all the gas flows in five years, the weak correlation between the time series is shown but stronger than that in a single year. It means the trend in the early years are similar with the future trends. Compared with other systems in nature and industry, the power law of NGPS is not as obvious and accurate as others, as seen in Fig. 37, except for the characteristics described above, the kind and amount of data for analysis also have effects.

4. Conclusion and recommendation

This paper analyzes the characteristics of NGPS, which shows the NGPS is atypical small world network and has atypical SOC properties.

The NGPS is basically close to a small world network, but the structural characteristics of NGPS itself allow for differences between that and traditional small world network. The dendritic structure of the network increases the average path length of the network as a whole, which also has a low aggregation effect. However, the NGPS construction process is influenced by a combination of economic and

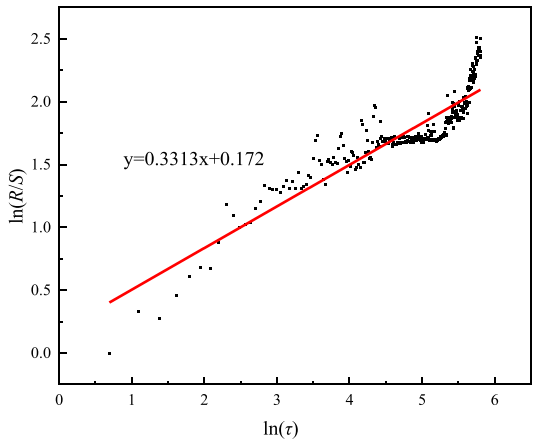

(a) 2017

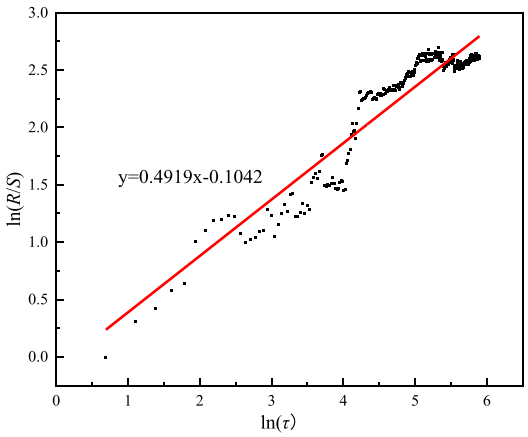

(b) 2018

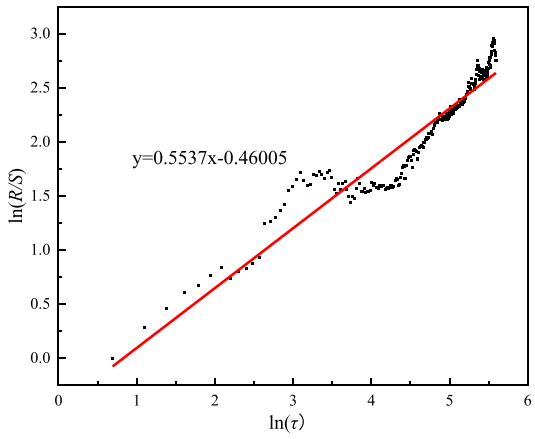

(c) 2019

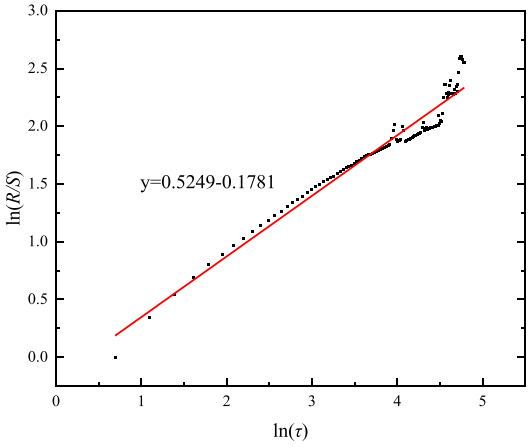

(d) 2020

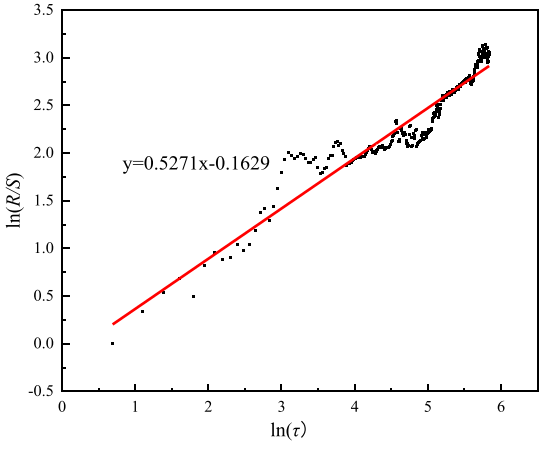

(e) 2021

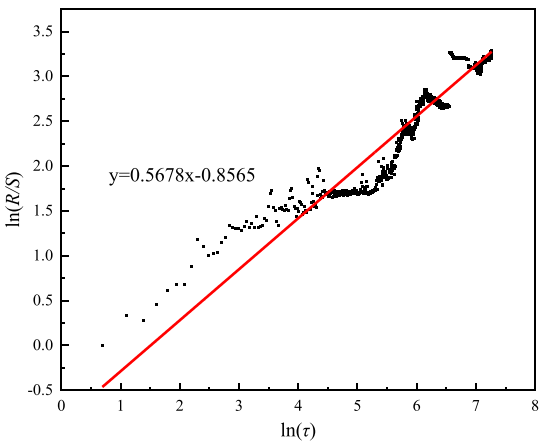

(f) five years

Fig. 36. R/S fitting line in different years.

Table 22
Parameters of R/S fitting line.

year	H	a	C	R^2
2017	0.3313	1.4943	-0.2085	0.8060
2018	0.4919	1.2672	-0.0111	0.8855
2019	0.5537	0.9266	0.0773	0.9026
2020	0.5249	1.2041	0.0351	0.9477
2021	0.5271	1.2245	0.0383	0.9096
five years	0.5687	0.6298	0.1000	0.8926

geographical factors, which can offset the low aggregation effect of the dendritic network structure. The combined effect of these factors result NGPS with small world characteristics, but with a larger mean path than a standard small world network and an aggregation factor close to that of a standard small world network, which is defined as atypical small world network.

The SOC in NGPS can be called atypical SOC, which fits the power law between scale and frequency in a special range. For NGPS, the data of gas flows which mean the system function, has the properties of concentration and periodicity. The reasons for the periodicity are the main affecting components like season changing and special holidays, which are periodical. The reasons for the concentration are the importance and status of NGPS, which bring the stableness of its operations, also force the development of SCADA and the internal detection technology to protect NGPS. In addition, the presence of line-pack and block valves bring the time lags to NGPS and prevent the cascade failures.

The data for analysis is the calorific values equally transformed from natural gas which is to show the operation function of NGPS, so it is indirect to research the scale of failure. Since the accident data metering and gathering of NGPS is not as perfect as power grid system, the amount of the data for analysis is not enough to fully get the corresponding events frequencies.

For NGPS managers and operators, the atypical properties of NGPS also prove and explain that:

- the NGPS has the similar characteristics with the Heinrich accident triangle(Jehring and Heinrich, 1951);
- if the major accident is prevented, it is necessary to reduce the overall probability of all kinds of accidents. The methods to reduce overall probability of accidents are more reliable and effective such as using pipes of higher grade of steel, developing more perfect SCADA and performing internal testing regularly. In addition, the digital twin technology in NGPS and uav line patrol also can support the increase of NGPS overall safety;
- since NGPS is a closed system with high pressure, the state of the NGPS can be in critical state anytime, which can not be ignored corresponding to the higher or lower pressure, or to the kinds of disturbance;

The R/S analysis proves that the data of NGPS in the past and future has weak correlation in time series, and the temporal granularity can affect the R/S results of NGPS. In the view of longer time series, the Hurst index show the yearly trend are positively correlated. Combined with the SOC analysis, the results prove that the critical state transformation is independent from the types of the events, which also prove the atypical characteristics.

In the future, it is important and necessary to build the historical database for the real NGPS accidents, especially for the index which can directly evaluate the scale of the accidents. In this way, the SOC characteristics of NGPS will be analyzed more accurately. The human factors are the main components which result in the disturbances on NGPS with high uncertainty, so it is necessary to research the corresponding area and focus more on the related training on staff for NGPS. Complex network theory is supposed to developed for the special system like NGPS, based on its atypical network propoties.

CRediT authorship contribution statement

HE Qian: Visualization, Validation. **Faber Michael Havbro:** Validation, Supervision. **ZIO Enrico:** Writing – review & editing,

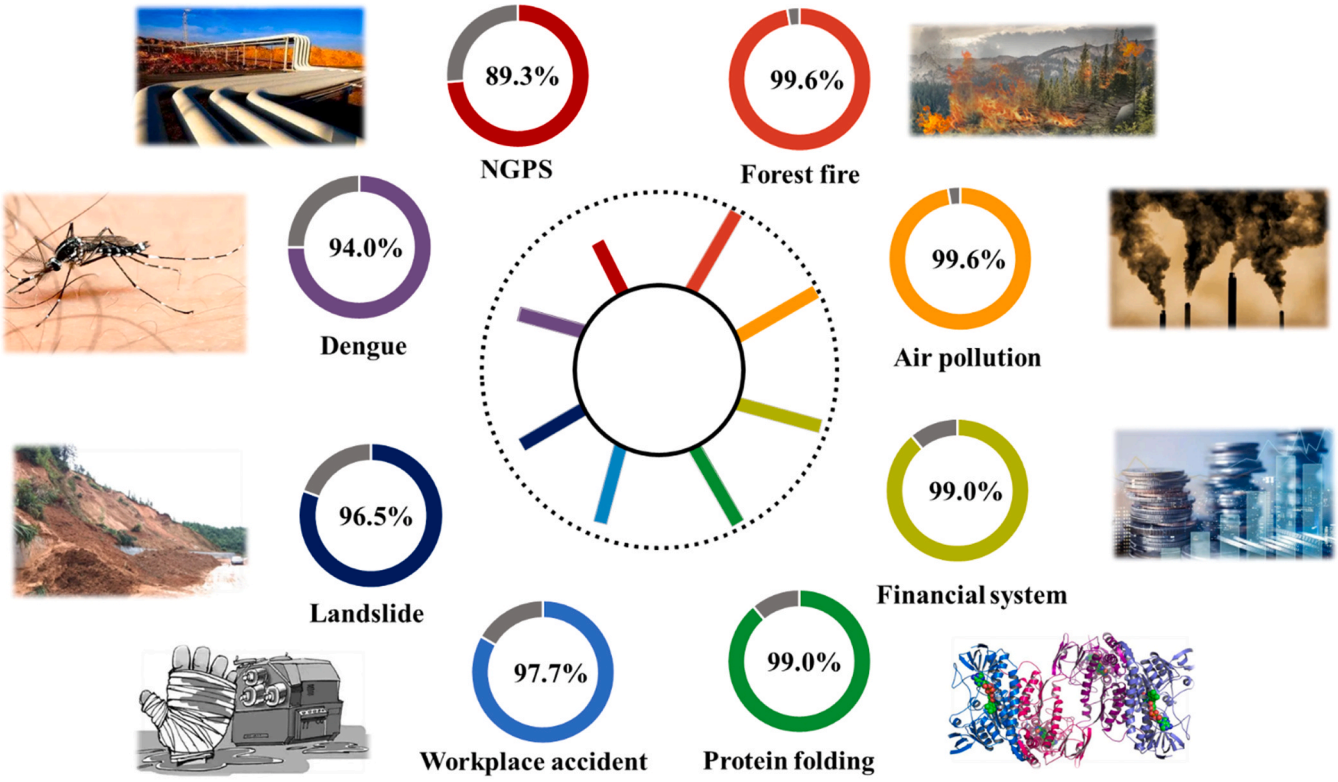

Fig. 37. Systems and corresponding SOC properties.

Supervision. **Su Huai:** Supervision, Project administration, Funding acquisition. **Zhang Jinjun:** Writing – review & editing, Supervision. **Yang Zhaoming:** Writing – original draft, Validation, Investigation, Formal analysis, Conceptualization. **Xiang Qi:** Writing – review & editing, Investigation, Conceptualization.

Declaration of Competing Interest

We declare that we have no financial and personal relationships with other people or organizations that can inappropriately influence our work, there is no professional or other personal interest of any nature or kind in any product, service and/or company that could be construed as influencing the position presented in, or the review of, the manuscript entitled, "The Atypical Transport System: Natural Gas Pipeline System".

Data Availability

Data will be made available on request.

Acknowledgements

This work is supported by National Natural Science Foundation of China [grant number 51904316], and the research fund provided by China University of Petroleum, Beijing [grant number 2462021YJRC013]. We appreciate the contributions of the editors and reviewers to the improvement of this work.

References

Adamic, L.A., Huberman, B.A., 2000. Power-law distribution of the world wide web, 2115–2115 Sci. (80-.) 287. https://doi.org/10.1126/science.287.5461.2115a.
Albert, R., Barabási, A.L., 2000. Topology of evolving networks: local events and universality. Phys. Rev. Lett. 85, 5234–5237. https://doi.org/10.1103/PhysRevLett.85.5234.
Albert, R., Albert, I., Nakarado, G.L., 2004. Structural vulnerability of the North American power grid. Phys. Rev. E - Stat. Nonlinear, Soft Matter Phys. 69, 1–4. https://doi.org/10.1103/PhysRevE.69.025103.
Amaral, L.A.N., Scala, A., Barthélémy, M., Stanley, H.E., 2000. Classes of small world networks. Proc. Natl. Acad. Sci. U. S. A. 97, 11149–11152. https://doi.org/10.1073/pnas.200327197.
American, S., America, N., American, S., 1991. Self-organized criticality, 264, 46–53.
Bak, P., 1990. Self-organized criticality. Phys. A Stat. Mech. Appl. 163, 403–409.
Bak, P., Tang, C., Wiesenfeld, K., 1987. Self-organized criticality: an explanation of the 1/f noise. Phys. Rev. Lett. 59, 381–384. https://doi.org/10.1103/PhysRevLett.59.381.
Bak, P., Tang, C., Wiesenfeld, K., 1988. Self-organized criticality. Phys. Rev. A 38, 364–374. https://doi.org/10.1103/PhysRevA.38.364.
Barabā, A.L., Barabási, A.-L., Jeong, H., Néda, Z., Ravasz, E., Schubert, A., Vicsek, T., 2002. Evolution of the social network of scientific collaborations. Phys. A Stat. Mech. Appl. 311, 590–614.
Barabási, A.L., Albert, R., 1999. Emergence of scaling in random networks. Science 286, 509–512. https://doi.org/10.1126/science.286.5439.509.
Barrat, A., Weigt, M., 2011. On the properties of small world network models, 9781400841 Struct. Dyn. Netw. 321–334. https://doi.org/10.1515/9781400841356.321.
Bernardes, A.T., Moreira, J.G., 1995. Self-organized criticality in a model for fracture on fibrous materials. J. Phys. I 5, 1135–1141. https://doi.org/10.1051/jp1:1995187.
Bhattacharya, K., Manna, S.S., 2007. Self-organized critical models of earthquakes. Phys. A Stat. Mech. Appl. 384, 15–20. https://doi.org/10.1016/j.physa.2007.04.106.
Boccaletti, S., et al., 2006. Complex networks: structure and dynamics. Phys. Rep. 175–308. https://doi.org/10.1016/j.physrep.2005.10.009.
Caldarelli, G., Marchetti, R., Pietronero, L., 2000. The fractal properties of Internet. Europhys. Lett. 52, 386–391. https://doi.org/10.1209/epl/i2000-00450-8.
Camacho, J., Guimerà, R., Amaral, L.A.N., 2002a. Analytical solution of a model for complex food webs. Phys. Rev. E - Stat. Phys., Plasmas, Fluids, Relat. Interdiscip. Top. 65, 1–4. https://doi.org/10.1103/PhysRevE.65.030901.
Camacho, J., Guimerà, R., Nunes Amaral, L.A., 2002b. Robust patterns in food web structure. Phys. Rev. Lett. 88, 4. https://doi.org/10.1103/PhysRevLett.88.228102.
Carreras, B.A., Lynch, V.E., Dobson, I., Newman, D.E., 2002. Critical points and transitions in an electric power transmission model for cascading failure blackouts. Chaos 12, 985–994. https://doi.org/10.1063/1.1505810.
Chenhui, S., Jun, X., Guoqiang, Z., Ziyuan, H., Xinsong, Z., 2021. Security region of natural gas pipeline network system: concept, method and application. Energy 217, 1–14. https://doi.org/10.1016/j.energy.2020.119283.
Chessa, A., Marinari, E., Vespignani, A., 1998. Energy constrained sandpile models. Phys. Rev. Lett. 80, 4217–4220. https://doi.org/10.1103/PhysRevLett.80.4217.
Clar, S., Drossel, B., Schenk, K., Schwabl, F., 1999. Self-organized criticality in forest-fire models. Phys. A Stat. Mech. Appl. 266, 153–159. https://doi.org/10.1016/S0378-4371(98)00587-1.
Da Cruz, J.P., Lind, P.G., 2012. Self-organized criticality in a network of economic agents with finite consumption. Phys. A Stat. Mech. Appl. 391, 1445–1452. https://doi.org/10.1016/j.physa.2011.11.012.
De Arcangelis, L., Herrmann, H.J., 2002. Self-organized criticality on small world networks. Phys. A Stat. Mech. Appl. 308, 545–549. https://doi.org/10.1016/S0378-4371(02)00549-6.
Dorogovtsev, S.N., Goltsev, A.V. and Mendes, J.F.F. (2007) 'Critical phenomena in complex networks'. pp.1–79.https://doi.org/10.1103/RevModPhys.80.1275.
Dunne, J.A., Williams, R.J., Martinez, N.D., 2002. Food-web structure and network theory: the role of connectance and size. Proc. Natl. Acad. Sci. U. S. A. 99, 12917–12922. https://doi.org/10.1073/pnas.192407699.
Dupoyet, B., Fiebig, H.R., Musgrove, D.P., 2010. Gauge invariant lattice quantum field theory: Implications for statistical properties of high frequency financial markets. Phys. A Stat. Mech. Appl. 389, 107–116. https://doi.org/10.1016/j.physa.2009.09.002.
Dupoyet, B., Fiebig, H.R., Musgrove, D.P., 2011. Replicating financial market dynamics with a simple self-organized critical lattice model. Phys. A Stat. Mech. Appl. 390, 3120–3135. https://doi.org/10.1016/j.physa.2011.04.017.
Ebrahem, F., Bamer, F., Markert, B., 2020. Origin of reversible and irreversible atomic-scale rearrangements in a model two-dimensional network glass. Phys. Rev. E 102. https://doi.org/10.1103/PhysRevE.102.033006.
Entsog, 2021. ⟨https://www.entsog.eu⟩.
Feigenbaum, J., 2003. Financial physics. Rep. Prog. Phys. 66, 1611–1649. https://doi.org/10.1088/0034-4885/66/10/R02.
Fell, D.A., Wagner, A., 2011. The small world of metabolism, 9781400841 Struct. Dyn. Netw. 215–216. https://doi.org/10.1515/9781400841356.215.
Heider, Y., Bamer, F., Ebrahem, F., Markert, B., 2022. Self-organized criticality in fracture models at different scales. Ex. Count. 2, 100054 https://doi.org/10.1016/j.exco.2022.100054.
Hoffmann, H., Payton, D.W., 2014. Suppressing cascades in a self-organized-critical model with non-contiguous spread of failures. Chaos, Solitons Fractals 67, 87–93. https://doi.org/10.1016/j.chaos.2014.06.011.
Huang, P.Y., Kurasch, S., Alden, J.S., Shekhawat, A., Alemi, A.A., McEuen, P.L., Sethna, J.P., Kaiser, U., Muller, D.A., 2013. Imaging atomic rearrangements in two-dimensional silica glass: watching silica's dance. Science 342, 224–227. https://doi.org/10.1126/science.1242248.
Hurst, H.E., 1951. Long-term storage capacity of reservoirs. Trans. Am. Soc. Civ. Eng. 116, 770–799. https://doi.org/10.1061/taceat.0006518.
Jehring, J., Heinrich, H.W., 1951. Industrial accident prevention: a scientific approach. Ind. Labor Relat. Rev. 4, 609. https://doi.org/10.2307/2518508.
Jensen, H.J., Magnasco, M.O., 1999. Self-organized criticality: emergent complex behavior in physical and biological systems. Phys. Today 52 (10), 76–78. https://doi.org/10.1063/1.882869.
Jeong, H., Tombor, B., Albert, R., Oltval, Z.N., Barabásl, A.L., 2000. The large-scale organization of metabolic networks. Nature 407, 651–654. https://doi.org/10.1038/35036627.
Jun, X., Yuqing, Q., Buxin, S., Chenhui, S., 2023. Operational boundary of flow network. Reliab. Eng. Syst. Saf. 231, 1–17. https://doi.org/10.1016/j.ress.2022.108974.
Kato, A., Thau, D., Hudak, A.T., Meigs, G.W., Moskal, L.M., 2020. Quantifying fire trends in boreal forests with Landsat time series and self-organized criticality. Remote Sens. Environ. 237, 111525 https://doi.org/10.1016/j.rse.2019.111525.
Li, J.F., Zhang, B.H., Liu, Y.F., Wang, K., Wu, X.S., 2012. Spatial evolution character of multi-objective evolutionary algorithm based on self-organized criticality theory. Phys. A Stat. Mech. Appl. 391, 5490–5499. https://doi.org/10.1016/j.physa.2012.06.032.
Lu, D., Du, S., 2007. Regulating economic systems in a multi-trait model of self-organized criticality. Phys. A Stat. Mech. its Appl. 373, 586–592. https://doi.org/10.1016/j.physa.2006.04.122.
Marković, D., Gros, C., 2014. Power laws and self-organized criticality in theory and nature. Phys. Rep. 536, 41–74. https://doi.org/10.1016/j.physrep.2013.11.002.
Mauro, J.C., Diehl, B., Marcellin, R.F., Vaughn, D.J., 2018. Workplace accidents and self-organized criticality. Phys. A Stat. Mech. its Appl. 506, 284–289. https://doi.org/10.1016/j.physa.2018.04.064.
Milovanov, A.V., Rasmussen, J.J., Groslambert, B., 2021. Black swans, extreme risks, and the e-pile model of self-organized criticality. Chaos, Solitons Fractals 144, 110665. https://doi.org/10.1016/j.chaos.2021.110665.
Moret, M.A., 2011. Self-organized critical model for protein folding. Phys. A Stat. Mech. Appl. 390, 3055–3059. https://doi.org/10.1016/j.physa.2011.04.008.
Najafi, M.N., Tizdast, S., 1999. Self-organized criticality.
Newman, M.E.J., 2001. From the Cover: the structure of scientific collaboration networks. Proc. Natl. Acad. Sci. 98, 404–409. https://doi.org/10.1073/pnas.021544898.
Nielsen, K.J., 2014. Improving safety culture through the health and safety organization: a case study. J. Saf. Res. 48, 7–17. https://doi.org/10.1016/j.jsr.2013.10.003.
Onody, R.N., De Castro, P.A., 2003. Optimization and self-organized criticality in a magnetic system. Phys. A Stat. Mech. its Appl. 322, 247–255. https://doi.org/10.1016/S0378-4371(02)01816-2.
Paczuski, M., Hughes, D., 2004. A heavenly example of scale-free networks and self-organized criticality. Phys. A Stat. Mech. its Appl. 342, 158–163. https://doi.org/10.1016/j.physa.2004.04.073.
Pastor-Satorras, R., Vázquez, A., Vespignani, A., 2001. Dynamical and correlation properties of the internet, 258701-1-258701–4 Phys. Rev. Lett. 87. https://doi.org/10.1103/PhysRevLett.87.258701.

Pázmándi, F., Zaránd, G., Zimányi, G.T., 2000. Self-organized criticality in the hysteresis of the Sherrington-Kirkpatrick model. Phys. B Condens. Matter 275, 207–211. https://doi.org/10.1016/S0921-4526(99)00780-2.

Phillips, J.C., 2012. Frequency-rank correlations of rhodopsin mutations with tuned hydropathic roughness based on self-organized criticality. Phys. A Stat. Mech. Appl. 391, 5473–5478. https://doi.org/10.1016/j.physa.2012.06.020.

Poon, S.H., Granger, C.W.J., 2003. Forecasting volatility in financial markets: a review. J. Econ. Lit. 41, 478–539. https://doi.org/10.1257/jel.41.2.478.

Redner, S., 1998. How popular is your paper? An empirical study of the citation distribution. Eur. Phys. J. B 4, 131–134. https://doi.org/10.1007/s100510050359.

Saba, H., Miranda, J.G.V., Moret, M.A., 2014. Self-organized critical phenomenon as a q-exponential decay - avalanche epidemiology of dengue. Phys. A Stat. Mech. Appl. 413, 205–211. https://doi.org/10.1016/j.physa.2014.06.045.

Sethna, J.P., 2022. Power laws in physics. Nat. Rev. Phys. 4, 501–503. https://doi.org/10.1038/s42254-022-00491-x.

Shannon, H.S., Mayr, J., Haines, T., 1997. Overview of the relationship between organizational and workplace factors and injury rates. Saf. Sci. 26, 201–217. https://doi.org/10.1016/S0925-7535(97)00043-X.

Shi, K., Liu, C.Q., 2009. Self-organized criticality of air pollution. Atmos. Environ. 43, 3301–3304. https://doi.org/10.1016/j.atmosenv.2009.04.013.

Song, W., Weicheng, F., Binghong, W., Jianjun, Z., 2001. Self-organized criticality of forest fire in China. Ecol. Modell. 145, 61–68. https://doi.org/10.1016/S0304-3800(01)00383-0.

Strogatz, S.H., 2001. Exploring complex networks. Nature 6825 (410), 268. https://doi.org/10.1038/35065725.

Telesford, Q.K., Joyce, K.E., Hayasaka, S., Burdette, J.H., Laurienti, P.J., 2011. The ubiquity of small world networks. Brain Connect 1, 367–375. https://doi.org/10.1089/brain.2011.0038.

Turcotte, D.L., Malamud, B.D., 2004. Landslides, forest fires, and earthquakes: examples of self-organized critical behavior. Phys. A Stat. Mech. Appl. 340, 580–589. https://doi.org/10.1016/j.physa.2004.05.009.

Turcotte, D.L., Rundle, J.B., 2002. Self-organized complexity in the physical, biological, and social sciences. Proc. Natl. Acad. Sci. U. S. A. 99, 2463–2465. https://doi.org/10.1073/pnas.012579399.

Williams, R.J., Berlow, E.L., Dunne, J.A., Barabási, A.L., Martinez, N.D., 2002. Two degrees of separation in complex food webs. Proc. Natl. Acad. Sci. U. S. A. 99, 12913–12916. https://doi.org/10.1073/pnas.192448799.

Zeng, H.L., Zhu, C.P., Wang, S.X., Guo, Y.D., Gu, Z.M., Hu, C.K., 2020. Scaling behaviors and self-organized criticality of two-dimensional small world neural networks. Phys. A Stat. Mech. Appl. 540, 123191 https://doi.org/10.1016/j.physa.2019.123191.

Zhang, G.Q., Wang, L., Chen, T.L., 2009. Analysis of self-organized criticality in weighted coupled systems. Phys. A Stat. Mech. Appl. 388, 1249–1256. https://doi.org/10.1016/j.physa.2008.12.043.

Zhao, X., Zhang, X., He, B., 2009. Study on self organized criticality of China power grid blackouts. Energy Convers. Manag. 50, 658–661. https://doi.org/10.1016/j.enconman.2008.10.002.